PLANT SCIENCES

Low ABA concentration promotes root growth and hydrotropism through relief of ABA INSENSITIVE 1-mediated inhibition of plasma membrane H+-ATPase 2

Rui Miao[1]*, Wei Yuan[1], Yue Wang[1], Irene Garcia-Maquilon[2], Xiaolin Dang[1], Ying Li[1], Jianhua Zhang[3], Yiyong Zhu[4], Pedro L. Rodriguez[2], Weifeng Xu[1]*

The *hab1-1abi1-2abi2-2pp2ca-1* quadruple mutant (*Qabi2-2*) seedlings lacking key negative regulators of ABA signaling, namely, clade A protein phosphatases type 2C (PP2Cs), show more apoplastic H+ efflux in roots and display an enhanced root growth under normal medium or water stress medium compared to the wild type. The presence of low ABA concentration (0.1 micromolar), inhibiting PP2C activity via monomeric ABA receptors, enhances root apoplastic H+ efflux and growth of the wild type, resembling the *Qabi2-2* phenotype in normal medium. *Qabi2-2* seedlings also demonstrate increased hydrotropism compared to the wild type in obliquely-oriented hydrotropic experimental system, and asymmetric H+ efflux in root elongation zone is crucial for root hydrotropism. Moreover, we reveal that *Arabidopsis* ABA-insensitive 1, a key PP2C in ABA signaling, interacts directly with the C terminus of *Arabidopsis* plasma membrane H+-dependent adenosine triphosphatase 2 (AHA2) and dephosphorylates its penultimate threonine residue (Thr[947]), whose dephosphorylation negatively regulates AHA2.

INTRODUCTION

Drought is the major threat to agricultural production on a worldwide scale. The plant root is the first organ to sense underground water stress and directs its growth toward moist soil (*1*, *2*). Modification of root system architecture (RSA) and tropisms is two sophisticated strategies in monocots and dicots to cope with water stress in soil (*3*). RSA consists of primary root and lateral roots, and lateral root formation is a key trait for exploring soil in search of nutrients and water. The availability of water across the circumferential axis of the root determines lateral root branching (*4–6*). Thus, the environmental inputs influence lateral root branching, and plants adapt RSA in response to different environmental stimuli (*7–9*). On the other hand, certain root tropisms, i.e., hydrotropism and xerotropism, enable guided root growth in soil under water deprivation. Hydrotropism enables roots to sense and chase soil moisture in any direction (*10*), whereas xerotropism indicates enhanced root downward growth guided by the gravity vector upon water stress (*11*). Crop roots must integrate RSA and root tropisms to survive in rainfed agriculture subjected to water scarcity environments.

Abscisic acid (ABA) is a critical stress hormone of plants, and the ABA signal transduction pathway has been well established in *Arabidopsis*. Pyrabactin resistance 1(PYR1)/PYR1-like (PYL)/ regulatory components of the ABA receptor (RCAR) protein family members (PYR/PYL/RCAR) were identified as soluble ABA receptors

(*12–14*), which inhibit, in an ABA-dependent manner, the clade A protein phosphatases type 2C (PP2Cs), such as the well-characterized ABA-insensitive 1 (ABI1), ABI2, hypersensitive to ABA1 (HAB1), and PP2CA (*15*). Sucrose non–fermenting-1–related protein kinase 2 protein kinases (SnRK2s) act as positive regulators in the ABA signal cascade, i.e., SnRK2.2, SnRK2.3, and open stomata 1 (OST1)/ SnRK2.6 (*12*, *16*). The cocrystal structures of different ABA receptors in complex with PP2Cs (such as ABI1 or HAB1) provide molecular insight into understanding how ABA-bound PYR/PYL receptors associate with PP2Cs and inhibit phosphatase activity (*13*, *17–20*). Thus, SnRK2s are relieved to phosphorylate downstream targets, such as various types of water and ion channels that determine turgor of guard cells and stomatal aperture or the basic leucine zippers (bZIPs) class transcription factors, to activate ABA response element (ABRE)–driven gene expression (*21–23*). In the absence of ABA, PYR/PYL/RCARs do not efficiently bind and inhibit PP2Cs. Thus, PP2Cs interact with and suppress the kinase activity of SnRK2s through dephosphorylation of the kinase activation loop and thereby repress ABA signaling (*12*, *13*, *16*, *17*, *20*).

It has been found that ABA signaling is required for root hydrotropism in *Arabidopsis* (*24*, *25*). The *aba1-1* and *abi2-1* mutant seedlings are less capable of responding to moisture gradients, whereas application of ABA to *aba1-1* restored normal sensitivity to the hydrotropic stimulus (*26*). The root of *no hydrotropic response 1* (*nhr1*) mutant was less sensitive to ABA (*27*), and ABA up-regulates the expression of *mizu-kussei 1* (*miz1*), a gene essential for hydrotropism (*28*). *112458*, a sextuple *PYR/PYL* mutant, displayed a negligible hydrotropic response, whereas *Qabi2-2* plants, a *pp2cs* quadruple mutant, exhibited enhanced hydrotropism (*24*). Recent studies found that the SnRK2s regulate hydrotropic response in cortical cells of the elongation zone (*25*). These findings suggest that hydrotropism depends on the core ABA signal transduction pathway (PYR/PYL/RCAR-PP2Cs-SnRK2s). In addition, Planes *et al.* (*29*) reported that SnRK2.2, but not OST1/SnRK2.6, phosphorylates

[1]Center for Plant Water-Use and Nutrition Regulation and College of Life Sciences, Joint International Research Laboratory of Water and Nutrient in Crops, Fujian Agriculture and Forestry University, Jinshan Fuzhou 350002, China. [2]Instituto de Biología Molecular y Celular de Plantas, Consejo Superior de Investigaciones Científicas–Universidad Politecnica de Valencia, ES-46022 Valencia, Spain. [3]Department of Biology, Hong Kong Baptist University, and State Key Laboratory of Agrobiotechnology, Chinese University of Hong Kong, Hong Kong. [4]Jiangsu Collaborative Innovation Center for Solid Organic Waste Resource Utilization, College of Resources and Environmental Science, Nanjing Agricultural University, Nanjing 210095, China. *Corresponding author. Email: ruimiao@fafu.edu.cn, miaorui2011@126.com (R.M.); wfxu@fafu.edu.cn (W.X.)

the C-terminal regulatory (R) domain of *Arabidopsis* plasma membrane (PM) H$^+$-dependent adenosine triphosphatase (ATPase) 2 (AHA2) in vitro, and application of 10 µM ABA suppressed 50% H$^+$ efflux from wild-type (WT) roots, leading to high inhibitory effect on root growth in *Arabidopsis*. Sustained ABA signaling led to dephosphorylation of AHA2, whereas the *Arabidopsis* ABI *abi1-1D* mutant did not exhibit ABA-induced inhibition of hypocotyl elongation (30). However, the molecular mechanisms governing these processes are not yet fully understood (31). For example, the mechanism by which core components of ABA signaling actually enhance *Arabidopsis* PM AHA phosphorylation or otherwise stimulate the proton pump activity is not known.

Several Thr and Ser residues clustered within the 100–amino acid–long C-terminal R domain of *Arabidopsis* AHA are targets for posttranslational regulation (32, 33). The penultimate threonine residue (Thr^{947}) of AHA2 plays a crucial role in regulating AHA activity and is a major auxin-induced phosphorylation site (34, 35). 14-3-3 protein binds to phosphorylated Thr^{947} of AHA2 and stimulates AHA activity (36–41). On the other hand, SOS2-like protein kinase 5 (PKS5), a Ser/Thr protein kinase, phosphorylates Ser^{931} in the C terminus of AHA2, which prevents the interaction of AHA2 with 14-3-3 protein and impairs AHA activity (42–44). The *aha2* mutant showed shorter primary root and lateral root length than WT Columbia-0 (Col-0) in response to various treatments with different nitrogen concentrations (45). Transgenic plants overexpressing *AHA1* show impaired ABA-induced stomatal closure (46). Constitutive expression of *Arabidopsis* AHA2 using the specific guard cell promoter *GC1* enhances light-induced stomatal opening and promotes plant growth (47).

Previously, we reported that brassinosteroid (BR)–insensitive 1 (BRI1), a BR receptor, targets AHA2 and AHA7 to mediate hydrotropic response in *Arabidopsis*, and a *bri1-5* mutant showed reduced root curvature in the hydrotropism assay, which correlates with lower apoplastic H$^+$ extrusion (48, 49). Here, we demonstrate that ABI1, a key component of clade A PP2Cs in ABA signal transduction pathway, directly interacts with the C-terminal R domain of AHA2 and dephosphorylates Thr^{947}, which decreases PM H$^+$ extrusion and negatively regulates primary root growth and hydrotropic response.

RESULTS

Effects of ABA supplies on root growth of Col-0 under normal growth conditions or water potential gradient assays
We used a water stress medium, one-half–strength Hoagland medium supplemented with 0.3% (v/v) glycerol and 0.06% (w/v) alginic acid, modified from the water potential gradient assay originally established by Saucedo *et al.* (50), to generate a vertical gradient where the upper part of the plate has a lower water potential than the lower part. The water stress medium assay was designed to imitate a soil moisture gradient under field conditions (48) and to study the role of ABA signaling in regulating root growth of seedlings subjected to water stress. To establish whether the designed water stress medium assay is a reliable system to study *Arabidopsis* roots in response to water stress, we analyzed a group of well-characterized ABA-related mutants. Thus, two ABA biosynthetic mutants (*aba1-1* and *aba2-1*), the sextuple mutant impaired in six ABA receptors (*pyr1pyl1pyl2pyl4pyl5pyl8*, abbreviated as *112458*), the *hab1-1abi1-2abi2-2pp2ca-1* quadruple mutant (*Qabi2-2*), and the ABA catabolic
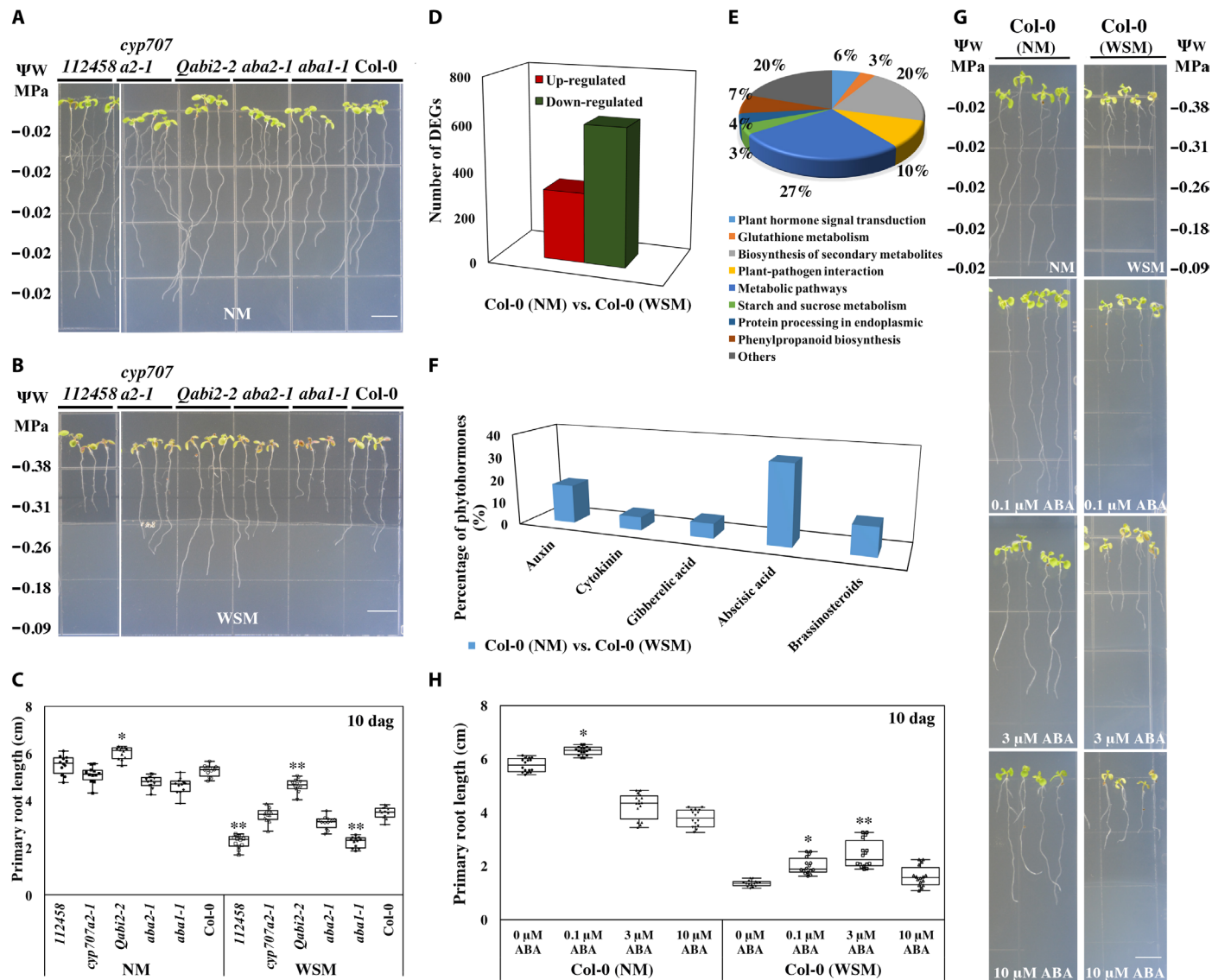
mutant *cyp707a2-1* were assayed under water stress medium (Fig. 1, A and C) (51–55). As expected, *aba1-1* and *112458* loss-of-function mutants showed notably shorter root compared to WT Col-0, and the mutant lacking negative regulators of ABA signaling (*Qabi2-2*) exhibited significantly longer roots compared to the WT under water stress medium (Fig. 1, B and C). These results confirm that water stress medium is sufficient to investigate *Arabidopsis* root growth under water stress.

Next, we performed high-throughput RNA sequencing (RNA-seq) by an Illumina HiSeq 2000 platform using *Arabidopsis* WT Col-0 root tips as materials (<5 mm from the root cap), including the root cap, meristem, and elongation zone. More than 47 million–base pair clean reads were mapped onto the *Arabidopsis* genome sequence, and expression of at least 25,900 genes was detected in root tips of Col-0 seedlings. A total of 912 differentially expressed genes (DEGs) were found in WT Col-0 seedlings grown in water stress medium (probability, >0.8) (56). Of these, 308 DEGs displayed higher expression, while 604 genes showed lower expression in water stress medium (Fig. 1D). Gene ontology analysis revealed genes involved in primary and secondary metabolism account for 54% DEGs (Fig. 1E). Considering that phytohormones are fundamental and widely involved in plant biological functions, we further analyzed the hormone-responsive DEGs. The mRNA-seq data revealed that hormone-responsive DEGs account for 6% of total DEGs. Of these, ABA-related genes account for more than 35% DEGs and showed that the higher percentage of DEGs among those genes are related to phytohormones in *Arabidopsis* (Fig. 1F). Together, these data verified that ABA signaling was important under water stress medium.
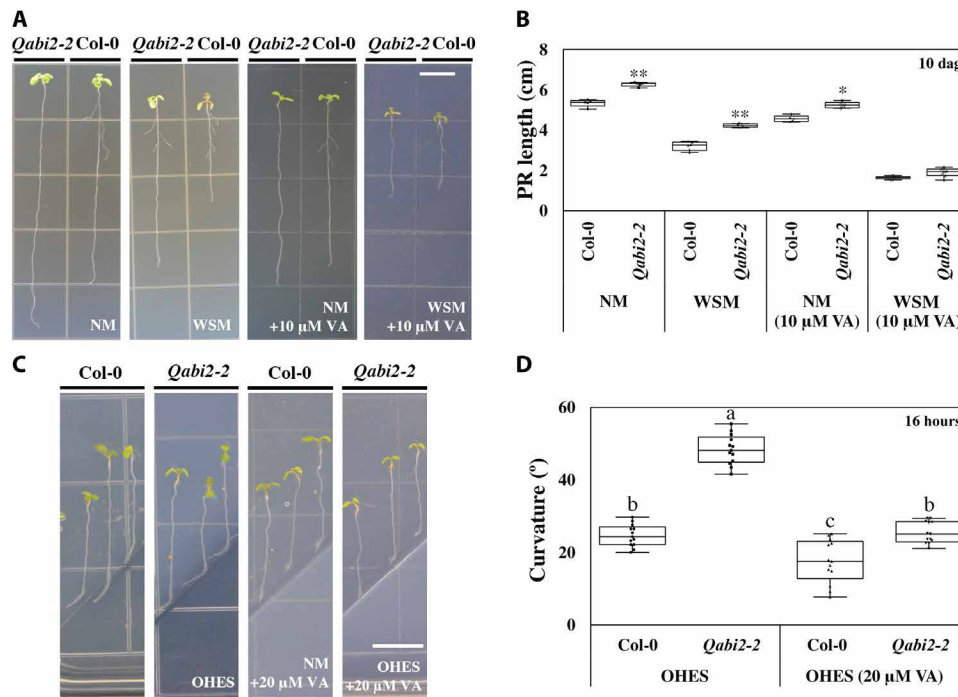
To analyze the effects of ABA on root growth of *Arabidopsis* WT Col-0 in normal medium and water stress medium, we performed root growth experiments in media supplemented with various concentrations of ABA. In normal medium, exogenous application of low ABA concentrations (0.1 µM) enhanced primary root elongation in WT, with in vivo ABA contents of 1.03 ± 0.21 ng/g for Col-0 and 2.60 ± 0.34 ng/g for Col-0 in the presence of 0.1 µM ABA, respectively, whereas 3 and 10 µM ABA impaired primary root growth, with in vivo ABA contents of 8.54 ± 0.82 ng/g for Col-0 in the presence of 3 µM ABA (Fig. 1, G and H, and table S1). Measurement of in vivo ABA content shows that a relatively minor (approximately 2.5-fold) increase in total ABA concentration can promote root growth, compared to Col-0 without ABA treatment. ABA transport is likely regulated, which explains that not all exogenous ABA is taken by the plant. However, 3 µM exogenous ABA treatment leads to approximately 8.5-fold increase in ABA content, which has a negative effect on root growth in normal medium. In water stress medium, both 0.1 and 3 µM ABA notably enhanced primary root growth of WT; therefore, an ABA effect on root growth depends on its concentrations and the water potential of the medium (Fig. 1, G and H).

Qabi2-2 seedlings show enhanced primary root growth and hydrotropic response
To explore the mechanism whereby the inactivation of PP2Cs leads to enhanced tolerance to water stress, we further studied a series of ABA-hypersensitive *pp2c* knockout mutants. Five days after germination (dag) seedlings of *pp2c* single mutant (*abi1-3*), triple mutants (*hab1-1abi1-2abi2-2* and *hab1-1abi1-2pp2ca-1*), and quadruple mutant *Qabi2-2 (hab1-1abi1-2abi2-2pp2ca-1)* plants were grown

Fig. 1. Effects of root growth in mutants from ABA signaling pathway and exogenous ABA application on root growth of *Arabidopsis* WT Col-0 seedlings upon a water potential gradient assay with mRNA-seq analysis. Growth phenotype of Col-0, *aba1-1*, *aba2-1*, *112458*, *cyp707a2-1*, and *Qabi2-2* seedlings grown on one-half–strength Hoagland medium [normal medium (NM)] (**A**) or one-half–strength Hoagland medium containing 0.3% (v/v) glycerol and 0.06% (w/v) alginic acid [water stress medium (WSM)] (**B**) for vertical growth lasting 5 days after which germinated for 5 days. (**C**) Measurement of primary root (PR) length of Col-0, *aba1-1*, *aba2-1*, *112458*, *cyp707a2-1*, and *Qabi2-2* seedlings shown in (A) and (B). Means ± SD ($n \geq 12$). *$P < 0.05$ and **$P < 0.01$ as determined by a Student's *t* test. (**D**) Number of DEGs in Col-0 (normal medium) versus Col-0 (water stress medium). Up-regulated and down-regulated genes are shown in red and green colors, respectively. (**E**) Pie chart showing the percentages of significant enrichment for biological process (BP) gene ontology terms in Col-0 (normal medium) versus Col-0 (water stress medium). (**F**) Bar charts showing the percentages of phytohormone-related DEGs in Col-0 (normal medium) versus Col-0 (water stress medium). (**G**) Col-0 seedlings [5 days after germination (dag)] grown on one-half–strength Murashige and Skoog (MS) medium were transferred and grown vertically on one-half–strength Hoagland medium without (left) or with 0.3% (v/v) glycerol and 0.06% (w/v) alginic acid (right) in the absence or presence of 0.1, 3, or 10 μM ABA for other 5 days. Scale bar, 10 mm. (**H**) Measurement of primary root length of Col-0 seedlings shown in (G). Error bars indicate ±SD ($n = 4$ in three independent experiments). *$P < 0.05$ and **$P < 0.01$ as determined by a Student's *t* test. Photo credit: Rui Miao, Fujian Agriculture and Forest University.

for 5 days in normal medium and water stress medium or 12 hours in a modified obliquely oriented hydrotropic experimental system to analyze root hydrotropism (fig. S1, A and B) (*24*, *46*). Compared to WT, the *Qabi2-2* seedlings showed enhanced primary root growth in normal medium and water stress medium. Root growth of *Qabi2-2* seedlings in normal medium resembled that of the WT in the presence of low ABA concentrations (0.1 μM), with in vivo ABA contents of

1.10 ± 0.77 ng/g (Figs. 1, G and H, and 2, A and B; and table S1). In water stress medium, primary root length of *Qabi2-2* seedlings was also significantly longer than that of Col-0 (Fig. 2, A and B), resembling Col-0 primary root growth in the presence of 0.1 and 3 μM ABA under water stress medium (Fig. 1, G and H).

It was previously reported that the *Qabi2-2* seedlings enhances *Arabidopsis* root hydrotropic response (*22*). We analyzed the

Fig. 2. Effects of sodium vanadate on root growth and curvature of Col-0 WT and *pp2cs* quadruple (*Qabi2-2*) mutant seedlings under water stress medium and obliquely oriented hydrotropic experimental system. (**A**) Five-dag Col-0 and *Qabi2-2* seedlings grown on one-half–strength MS were transferred and grown vertically on normal medium or water stress medium without or with 10 μM sodium vanadate (VA) for other 5 days. Scale bar, 10 mm. (**B**) Measurement of primary root length of Col-0 and *Qabi2-2* seedlings shown in (A). VA, a PM H⁺-ATPase inhibitor. (**C**) Photographs show that 5-dag Col-0 and *Qabi2-2* seedlings were transferred to split agar plates including 0.4 M D-sorbitol in the bottom with lower water potential [obliquely oriented hydrotropic experimental system (OHES)] for 16 hours in the absence or presence of 20 μM VA. (**D**) Root curvature angle shown in (C). Data are averages from three independent experiments. Error bars represent SD ($n = 6$). The asterisks indicate a significant difference based on the Student's *t* test (*$P < 0.05$ and **$P < 0.01$). Values with the same letters (a, b, or c) were not significantly different from one another [one-way analysis of variance (ANOVA), $P < 0.05$]. Photo credit: Rui Miao, Fujian Agriculture and Forest University.

hydrotropic responses of *pp2c* single mutant (*abi1-3*), triple mutant (*hab1-1abi1-2abi2-2*), and quadruple mutant *Qabi2-2* seedlings under an obliquely oriented hydrotropic experimental system (fig. S1B). The *Qabi2-2* seedlings showed the most sensitive hydrotropic response in an obliquely oriented hydrotropic experimental system, displaying the largest root bending angles (Fig. 2, C and D), whereas no significant differences in root curvature were detected among the WT, *abi1-3*, and *hab1-1abi1-2abi2-2* mutants (fig. S1B), suggesting that these genes might work redundantly in a dose-dependent manner. Given that gravitropism is the predominant tropic response that all other tropisms have to antagonize (*11*), we also analyzed the root gravitropic responses of the WT Col-0 and *Qabi2-2* seedlings in the absence or presence of low ABA concentration (0.1 μM). Nevertheless, in the absence or presence of low ABA concentration (0.1 μM), the root growth curvatures of the *Qabi2-2* seedling did not exhibit any notable differences compared to those of the Col-0 WT from the gravity vector during 8 or 16 hours (fig. S2, A and B).

Apoplastic H⁺ extrusion contributes to *Arabidopsis* primary root growth and the hydrotropic response

Apoplastic acidification results in cell wall loosening and facilitates cell elongation (*57*). To explain why the *Qabi2-2* plants showed enhanced primary root growth and hydrotropic response, we measured the apoplastic H⁺ efflux of primary root elongation zone in WT and *Qabi2-2* seedlings under normal medium, water stress medium, and obliquely oriented hydrotropic experimental system. In normal medium, the primary root elongation zone of 10-dag *Qabi2-2* seedlings exhibited significantly higher apoplastic H⁺ extrusion than WT (Fig. 3A), and the isolated PM vesicles from root cells of *Qabi2-2* seedlings showed higher H⁺ transport activity than those from WT roots as revealed by higher quenching of acridine orange [Absorbance (A)₄₉₂] in *Qabi2-2* seedlings compared to those of Col-0 WT (fig. S3A). As nitrate and azide suppress, respectively, tonoplast AHA and mitochondrial/chloroplastic adenosine 5′-triphosphate (ATP) hydrolase activity of F-ATPase (*58*, *59*), to avoid an underestimation of contamination by tonoplast, mitochondrial, and chloroplastic membrane in the isolated PM fractions, we analyzed nitrate-sensitive (50 mM; pH 8.0) and azide-sensitive (1 mM; pH 8.0) ATPase activity. The AHA activity displayed a negligible sensitivity to nitrate and azide, indicating that the obtained PM vesicles are pure (table S2). In contrast, the level of apoplastic H⁺ extrusion in the *Qabi2-2* seedlings was similar to that of the WT in medium supplemented with 0.1 μM ABA, whereas 10 μM ABA strongly impaired H⁺ extrusion in the WT (Fig. 3A). Both WT and *Qabi2-2* seedlings displayed notably higher apoplastic H⁺ extrusion in primary root in water stress medium and obliquely oriented hydrotropic experimental system compared to normal medium, suggesting that water stress stimulated apoplastic H⁺ extrusion in primary root (Fig. 3, B and C). However, apoplastic H⁺ efflux in lateral root of 10-dag *Qabi2-2* seedlings was not significantly different from the WT (fig. S4). This suggests that *Qabi2-2* plants have a different mechanism for primary root elongation and lateral root development in *Arabidopsis*.
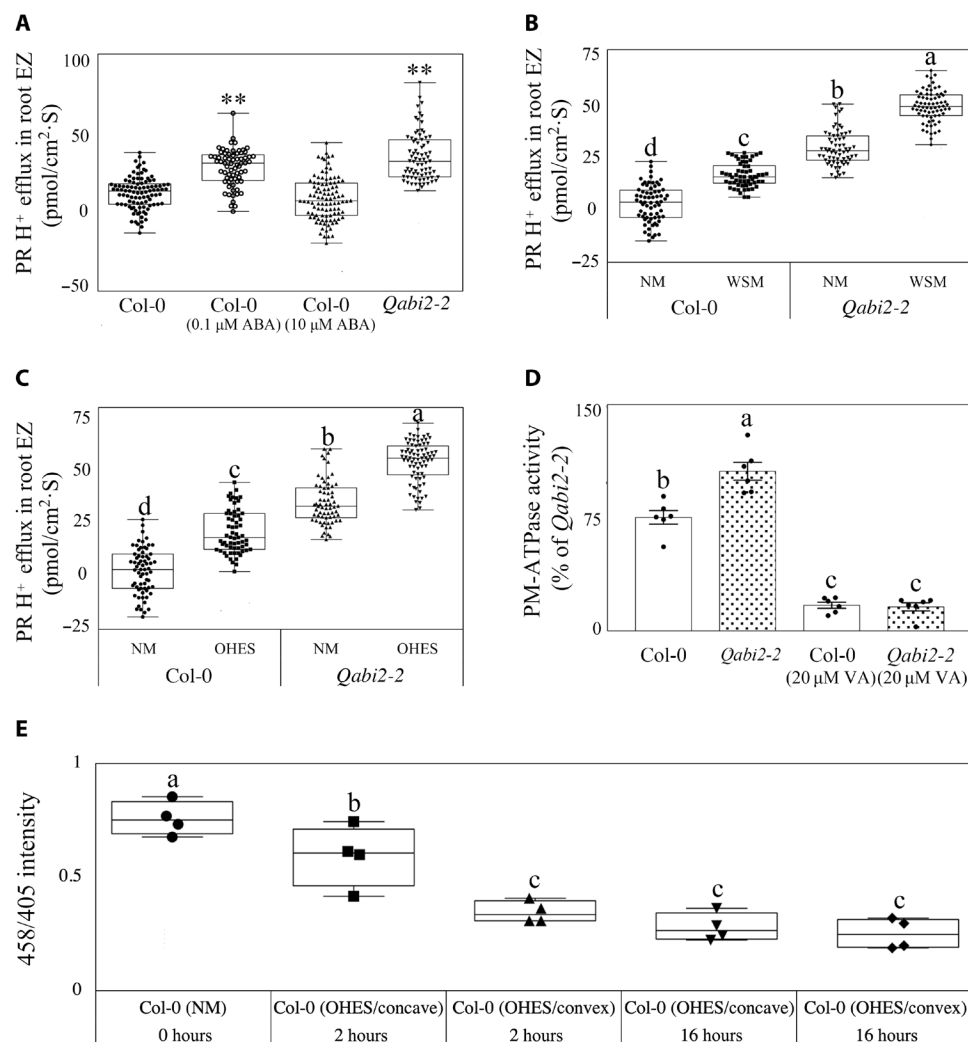
Fig. 3. H$^+$ efflux in roots of Col-0 WT and *Qabi2-2* seedlings. (**A**) H$^+$ efflux in primary root elongation zone (EZ) of Col-0 WT, Col-0 (0.1 μM ABA), Col-0 (10 μM ABA), and *Qabi2-2* mutant of these *Arabidopsis* plants was grown in normal medium. The values shown are the means, and error bars represent ±SD of six replicates from two independent experiments. The asterisks indicate a significant difference based on the Student's *t* test (**$P < 0.01$). (**B** and **C**) H$^+$ efflux in primary root elongation zone of Col-0 WT and *Qabi2-2* mutant of these *Arabidopsis* plants was grown in normal medium, water stress medium (B), or obliquely oriented hydrotropic experimental system (C). The values shown are the means, and error bars represent ±SD of six replicates from two independent experiments. (**D**) *Arabidopsis* PM AHA activity was measured in Col-0 WT and *Qabi2-2* seedlings in the absence or presence of 20 μM VA. PM vesicles were isolated from 10-dag Col-0 WT and *Qabi2-2* seedlings. The values shown are the means, and error bars represent ±SD of three replicates from two independent experiments. (**E**) Five-dag Col-0 WT roots transferred to normal medium or obliquely oriented hydrotropic experimental system lasting 2 or 16 hours were stained with 1 mM HPTS solution supplemented with 0.01% (v/v) Silwet L-77 for 30 min, and the root cells of elongation zone were visualized using the confocal (405- and 458-nm excitation wavelengths). The *y* axis represents the mean 458/405 values of the roots grown in normal medium or obliquely oriented hydrotropic experimental system lasting 2 or 16 hours. Error bars represent ±SD ($n = 4$). Values with the same letters (a, b, c, or d) were not significantly different from one another (one-way ANOVA, $P < 0.05$).

We reasoned that if apoplastic H$^+$ extrusion is crucial for primary root growth and hydrotropic response, then inhibition of AHA activity would result in decreased root growth and hydrotropic response. To this end, we performed a sodium vanadate (VA) treatment, which, at 20 μM, led to a marked inhibition of AHA activity from the isolated PM fractions of WT Col-0 and *Qabi2-2* roots (Fig. 3D). In the presence of 10 μM VA, primary root growth of 10-dag *Qabi2-2* seedlings was noticeably reduced in normal medium and water stress medium (Fig. 2A), and the primary root growth difference between WT and *Qabi2-2* seedlings was attenuated or abolished after 10 μM VA treatment in normal medium and water stress medium, respectively (Fig. 2B). Furthermore, application of

20 μM VA caused reduced root curvature in both the WT and the *Qabi2-2* seedlings for 12 or 16 hours in obliquely oriented hydrotropic experimental system (Fig. 2, C and D, and fig. S1B). Given that VA is not a specific inhibitor of PM AHA, we analyzed primary root growth of the *aha2* mutant (SALK_082786), which is impaired in a major PM AHA of the *Arabidopsis* AHA family (*48, 49*). Nine-dag seedlings of *aha2* showed shorter roots compared to the WT in water stress medium (fig. S1C), which suggests that the lower H$^+$ extrusion capability of *aha2* roots impairs primary root growth upon water stress medium (*57*). Moreover, we also analyzed the hydrotropic responses of *aha2* mutant (SALK_082786) under obliquely oriented hydrotropic experimental system during 6 and 16 hours

(fig. S1D), and the *aha2* mutant demonstrated a compromised hydrotropic response in obliquely oriented hydrotropic experimental system for 6 hours, showing significantly smaller root bending angles than those of Col-0 WT, whereas no notable differences in root curvature were observed between the WT and *aha2* mutant in obliquely oriented hydrotropic experimental system for 16 hours (fig. S1D).

As recent articles have reported that the asymmetric distributions of Ca^{2+} and cytokinin are required for root hydrotropism in *Arabidopsis* (*60*, *61*), we used 8-hydroxypyrene-1,3,6-trisulfonic acid trisodium salt (HPTS), a fluorescent pH indicator that penetrates the root apoplast but does not enter the root cells, to detect H^+ efflux in WT roots after hydrostimulated treatment (*62*). The protonated and deprotonated forms of HPTS dye were visualized with excitation wavelengths of 405 and 458 nm, respectively. Therefore, the 458/405 ratio value represents the apoplastic pH, and the lower 458/405 ratio means lower pH and more H^+ extrusion to apoplast. For example, fusicoccin treatment, which activates the PM AHAs, results in decreased 458/405 ratio values (*62*). The fluorescence of HPTS in the convex side displayed much lower 458/405 ratio values than that of the concave side of the bending root in obliquely oriented hydrotropic experimental system lasting 2 hours, reflecting a lower apoplastic pH in the convex side and suggesting that root curvature is conferred by asymmetric H^+ extrusion in the early stage (Fig. 3E and fig. S3, B to D). Moreover, WT roots in obliquely oriented hydrotropic experimental system for 16 hours displayed decreased 458/405 ratio values compared to those in normal medium, indicating that hydrotropic stimulus enhanced apoplastic acidification; however, the fluorescence of HPTS exhibited similar signal intensity values between the concave and the convex sides of the bending root in obliquely oriented hydrotropic experimental system lasting 16 hours, suggesting that the H^+ extrusion triggered root elongation of both the concave and the convex sides at a later stage (Fig. 3E and fig. S3, B to D). Together, we conclude that apoplastic H^+ extrusion across the PM in primary root contributes to root growth and hydrotropic response upon water stress.

ABI1 directly interacts with AHA2

To investigate how ABA signaling regulates apoplastic H^+ extrusion and AHA activity, we performed a split-ubiquitin yeast two hybrid (Y2H) assay to examine whether core components of the ABA signal transduction pathway directly interact with AHA2 (*63*). Full-length *PYR1*, *ABI1*, *SnRK2.2*, *SnRK2.3*, and *SnRK2.6* were cloned in pPR3-N prey vector, and full-length *AHA2* was cloned into pBT3-N bait vector. The respective combinations were cotransformed into the yeast strain NMY51, and only yeast colonies cotransformed with pBT3-N–ABI1 and pPR3-N–AHA2 showed visible growth after 3 days at 30°C in synthetically defined (SD) medium lacking adenine (Ade), leucine (Leu), tryptophan (Trp), and histidine (His) (SD-Leu-Trp-His-Ade) (Fig. 4A).

Next, to test whether the interaction of ABI1 with AHA2 actually occurs in planta, a bimolecular fluorescence complementation (BiFC) assay was performed in *Nicotiana benthamiana*, and a clear yellow fluorescent protein (YFP) fluorescence signal was detected when ABI1-cYFP and AHA2-nYFP were coexpressed in leaves (Fig. 4B). As controls, no interactions were detected in the combinations of the ABI1-cYFP with nYFP vector, AHA2-nYFP with cYFP vector, and nYFP vector with cYFP vector (Fig. 4B). The subcellular localization of ABI1 and AHA2 interaction was mainly observed at the PM (Fig. 4B).

ABI1 binds to the C-terminal R domain of AHA2 and dephosphorylates Thr^{947}

AHA2 comprises five intracellular domains: N terminus, A (actuator) domain, N (nucleotide-binding) domain, P (phosphorylation) domain, and a 100–amino acid–long C terminus (C100), namely, autoinhibitory domain or C-terminal R domain (Fig. 5A) (*31*, *32*). We cloned full-length *ABI1* in pGADT7 bait vector and the indicated *AHA2* domains, i.e., A domain, N domain, P domain, and C terminus (C100), in pGBKT7 prey vector. Then, we cotransformed the bait with each prey into the yeast strain AH109 and performed the Y2H growth assay. No interaction was observed between pGADT7-ABI1 and each of the following preys, i.e., pGBKT7-AHA2–A domain, N domain, or P domain, whereas the combination of pGADT7-ABI1 and pGBKT7–AHA2 (C100) conferred growth in SD-Leu-Trp-His-Ade medium, suggesting that ABI1 binds to the C-terminal R domain of AHA2 (Fig. 5B).

To validate the binding of ABI1 to AHA2 C terminus (C100) in planta, we further examined the combination of ABI1 and AHA2 C terminus (C100) using the firefly luciferase complementation imaging (LCI) assay. The results confirmed that the AHA2 C terminus (C100) can physically interact with ABI1 in *N. benthamiana* leaves (Fig. 5C). As controls, no luciferase signals were observed in the combinations of the ABI1-NLuc with CLuc vector, NLuc vector with CLuc–AHA2 (C100), or NLuc vector with CLuc vector, respectively (Fig. 5C).

The C terminus of AHA is referred to as an autoinhibitory domain or R domain, and phosphorylation of this domain is important for regulation of AHA activity (*31*). Specifically, auxin-induced phosphorylation of the penultimate residue (Thr^{947}) of AHA2 is crucial to activate AHA activity. To analyze whether ABI1 negatively regulates AHA activity through dephosphorylate of AHA2 in vivo, we coexpressed the combination of ABI–green fluorescent protein (GFP) and AHA2 (C100)–FLAG or GFP and AHA2 (C100)–FLAG in *N. benthamiana* leaves, respectively, and analyzed phosphorylation of Thr^{947} by immunoblot analysis using phospho–Thr^{947} ($pThr^{947}$) antibodies (*64*). Given the lability of $pThr^{947}$, we added *Arabidopsis* protein extracts containing *GRF6*, a member of the 14-3-3 gene family, to preserve $pThr^{947}$ during the analysis. The phosphorylation level of Thr^{947} in C100 was markedly lower when ABI1-GFP was coexpressed when compared to the GFP control. AHA protein abundance was similar in both cases, which suggests that ABI1-GFP dephosphorylates Thr^{947} in *N. benthamiana* leaf cells (Fig. 5D). However, AHA2 C terminus (C100) single-point mutations (T947A and T947D) generated by site-directed mutagenesis cannot prevent the interaction with ABI1 in the Y2H growth assay, suggesting that ABI1 binds to other amino acids of AHA2 (C100) to regulate phosphorylation of Thr^{947} (Fig. 5C).

AHA2 (C100)–FLAG expressed in *N. benthamiana* was purified by affinity chromatography and analyzed by mass spectrometry (MS). Our results show that the vicinity of Thr^{947} in AHA2 (C100)–FLAG does not have proper recognition sites for proteases and the expected small size of peptides including Thr^{947} could not be detected by MS (fig. S10). Different phosphoproteomic data obtained in vivo (http://phosphat.uni-hohenheim.de/phosphat.html) support phosphorylation of Thr^{947} in AHA2 (AT4G30190) (fig. S11), for instance, in response to osmotic stress and sucrose supply after sucrose starvation. Wu *et al.* (*65*) reported Thr^{947} phosphorylation of AHA2 and sucrose-induced phosphorylation of protein kinase SnRK2.5/SRK2H, which belongs to osmotic stress–activated subfamily I SnRK2s and is a close relative of SnRK2.2/2.3 (*66*).
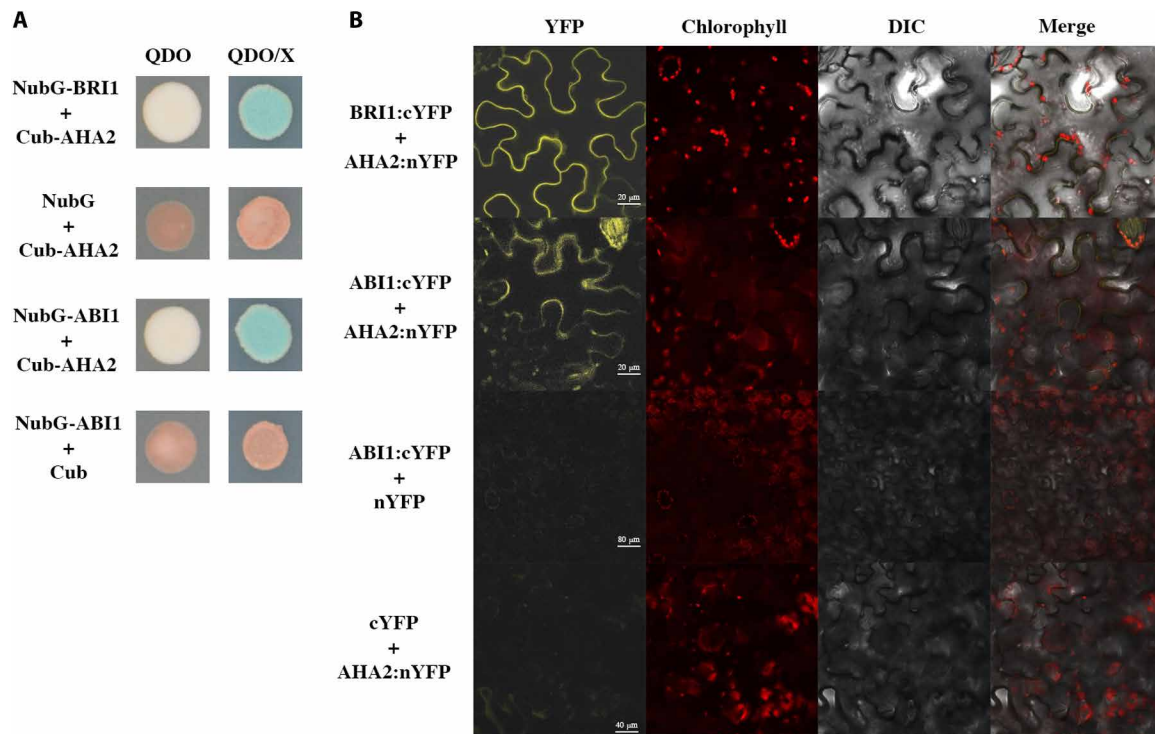
Fig. 4. Interaction of ABI1 with AHA2. (A) Split-ubiquitin Y2H assay showing the interaction between ABI1 and AHA2. QDO, quadruple dropouts; X, X-galactosidase; DIC, differential interference contrast. **(B)** Bimolecular fluorescence complementation (BiFC) assays showing in vivo interaction of ABI1 with AHA2 in tobacco (*N. benthamiana*) leaf epidermal cells.

Clade A PP2Cs negatively regulate AHA activity

There are 76 PP2Cs in the *Arabidopsis* genome, belonging to 10 subgroups (*67*). The well-known *ABI1*, *ABI2*, *HAB1*, and *PP2CA*, involved in the ABA signal transduction pathway, are clustered into clade A, which includes nine genes (*67*). Protein alignment shows that ABI1, ABI2, HAB1, and PP2CA are highly conserved, including the conserved tryptophan lock required for contact with ABA's ketone group (fig. S5A) (*67*). A cladogram analysis was conducted by Jalview 2.8.2 based on the average distance using percentage identity, showing that ABI1 and ABI2 group together, whereas HAB1 and PP2CA are separated (fig. S5B). We used BiFC assays again to detect the interactions of AHA2 with HAB1 and PP2CA in planta, respectively, and these two combinations display YFP signals after coexpressing in tobacco leaf cells, suggesting that HAB1 and PP2CA bind to AHA2 in plant cells as well (fig. S6).

Because of partially redundant function of PP2Cs, we observed no obvious difference in AHA activity and H$^+$ efflux in roots of 10-dag *abi1-3* mutant as compared to the WT (fig. S7, A and B). However, both AHA activity and H$^+$ efflux in roots of 10-dag *hab1-1abi1-2abi2-2* and *hab1-1abi1-2pp2ca-1* triple mutants and the *Qabi2-2* quadruple mutant seedlings were noticeably higher than those of WT in normal medium (Fig. 3D and fig. S7, A and B).

We analyzed the phosphorylation of Thr^{947} from isolated PM fractions of WT, *miz1*, and *Qabi2-2* seedlings by immunoblot analysis using pThr^{947} antibodies (*34*). Consistent with measurements of AHA activity, the phosphorylation level of Thr^{947} in *Qabi2-2* seedlings was higher than that of the WT and *miz1* mutant in normal medium, suggesting that combined loss-of-function PP2Cs led to increased phosphorylation of AHA2 and stimulation of H$^+$ extrusion

compared to WT and *miz1* (Fig. 6A and fig. S8A). Consistent with H$^+$ extrusion of the WT in the presence of 0.1 μM ABA in normal medium, the phosphorylation level of Thr^{947} in the WT and *miz1* treated with 0.1 μM ABA resembled *Qabi2-2* seedlings in the absence of ABA treatment (Fig. 6A and fig. S8A). As Moriwaki *et al.* (*28*) reported that ABA treatment never affect the hydrotropic phenotype of *miz1*, exogenous application of low ABA concentration (0.1 μM) did not enhance root curvature in *miz1* under obliquely oriented hydrotropic experimental system as well (fig. S8, B and C). These results suggest that low ABA concentrations can inhibit activity of PP2Cs phosphatases in WT and *miz1* and phenocopy the *Qabi2-2* seedling impairment of phosphatase activity and *MIZ1* might work downstream of core ABA signaling components (PYR/PYL/RCAR-PP2Cs) to mediate root hydrotropism.

Moreover, we analyzed ABI1 activity in vitro in the presence of PYL8, a major ABA receptor in root (*24*, *68*), at the indicated ABA concentrations (Fig. 6, B to D). The results show that submicromolar ABA concentrations are effective to inhibit ABI1 in the presence of PYL8; the half-maximal inhibitory concentration (IC$_{50}$) for ABI1 activity was 53 nM ABA, thereby disturbing interaction of ABI1 with C terminus of AHA2 and keeping Thr^{947} in the phosphorylated state for apoplastic H$^+$ extrusion. Higher ABA concentrations are effective in vitro to inhibit ABI1 (Fig. 6D), but in vivo treatment with high ABA concentrations induces up-regulation of PP2Cs transcripts and protein levels (*69*, *70*), whereas ABA receptors are down-regulated (*71*). As a result, sustained treatment with high ABA concentrations might lead to up-regulation of PP2Cs activity as a feedback mechanism to attenuate ABA signaling mediated by ABRE-binding factors (*69*, *70*).
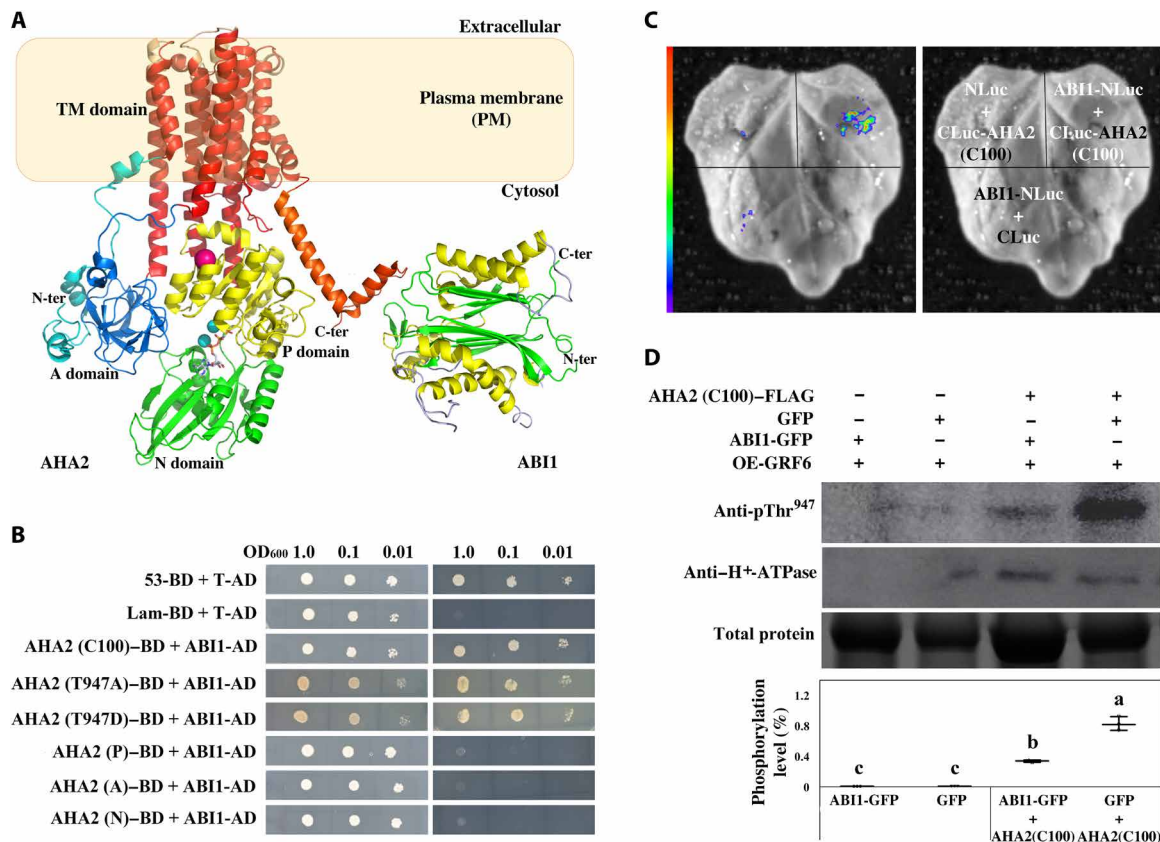
Fig. 5. ABI1 binds to C terminus of AHA2 and dephosphorylates Thr[947]. (**A**) Representative cartoon image showing the interaction of cytosolic ABI1 with homology modeling putative C terminus of AHA2 that located in PM. TM, transmembrane. (**B**) Y2H assay to detect the interaction of ABI1 with A domain, N domain, P domain, and AHA2 (C100). OD$_{600}$, optical density at 600 nm. AD, the activation domain; Lam, lamin; T, T-antigen; BD, the DNA binding domain. (**C**) The LCI images of *N. benthamiana* leaves coinfiltrated with the agrobacterial strain GV3101 containing the indicated fusion proteins. (**D**) In vivo dephosphatase assay examining the phosphorylation level of Thr[947] in the presence of ABI1–green fluorescent protein (GFP) or GFP, respectively. AHA2 (C100)–FLAG with ABI1-GFP or GFP were coexpressed in *N. benthamiana* leaves. The isolated PM fractions were mixed with extracts from *GRF6*–overexpressing (OE) transgenic *Arabidopsis* plants (AT5G10450), a member of the 14-3-3 family, to preserve pThr[947] during the analysis. The phosphorylation level of the Thr[947] in the C-terminal R domain of AHA was determined by immunoblot using anti–pThr[947] antibody. The phosphorylation level of AHA was quantified as the ratio of the signal intensity from the phosphorylated AHA to that from the amount of AHA2 (graph at middle). These assays were repeated at least three times with similar results. Values with the same letters (a and b) were not significantly different from one another (one-way ANOVA, $P < 0.05$).

DISCUSSION

In this work, we provide a molecular mechanism to explain the difference in root growth and hydrotropism between Col-0 WT and a series of mutants impaired in PP2Cs. Previously, it was reported that high-order loss-of-function *pp2c* mutants render partial constitutive response to endogenous ABA, and *pp2c* triple mutants exhibited partial up-regulation/down-regulation of ABA-responsive genes (*72*). In addition, our data clearly show that H$^+$ efflux across the PM at least partially contributes to the enhanced root growth and hydrotropic response in *pp2c* quadruple mutant *Qabi2-2* plants. Moreover, we identified which core components in the ABA signal transduction pathway interact with AHA2 and regulate AHA activity, thereby filling the gap between the ABA signal transduction pathway and PM AHA regulation concerning water stress–triggered H$^+$ extrusion.

Moderate water stress leads to ABA accumulation and causes H$^+$ efflux through root tips in *Arabidopsis* (*54*). Application of low ABA concentrations also triggers H$^+$ extrusion across the PM in *Arabidopsis* roots, whereas paradoxically high ABA concentrations abolish it (Fig. 3A). However, the molecular mechanisms that regulate this process are not fully understood. Previous studies

demonstrated that OST1/SnRK2.6 physically interacts, phosphorylates the K$^+$ uptake transporter 6, and balances potassium homeostasis in response to water stress (*73*). Similarly, OST1/SnRK2.6 phosphorylates and activates the PM transporters slow anion channel-associated 1 (SLAC1), a central guard cell S-type anion channel, to mediate ABA-induced stomatal closure (*74–76*), Conversely, the PP2C phosphatase ABI1 directly dephosphorylates SLAC1 N terminus and inhibits SLAC1 activity (*74*). SnRK2.2, rather than OST1/SnRK2.6 in vitro, phosphorylates the C terminus of AHA2, although this study lacks in vivo confirmation (*29*). Given that AHA2 is a PM protein, we used a split-ubiquitin system to analyze whether core ABA signaling components (PYR/PYL/RCAR-PP2Cs-SnRK2s) could bind to AHA2, thereby regulating PM AHA activity in response to ABA. Thus, we screened the possible interactions of AHA2 with the ABA receptor PYR1, PP2C ABI1, SnRK2.2, SnRK2.3, and SnRK2.6. Only ABI1 binding to AHA2 was observed in yeast, and the interaction of full-length AHA2 with ABI1 was confirmed in *N. benthamiana* leaf cells using the BiFC assay and Y2H and LCI assays; the interaction was mapped to the C terminus of AHA2.
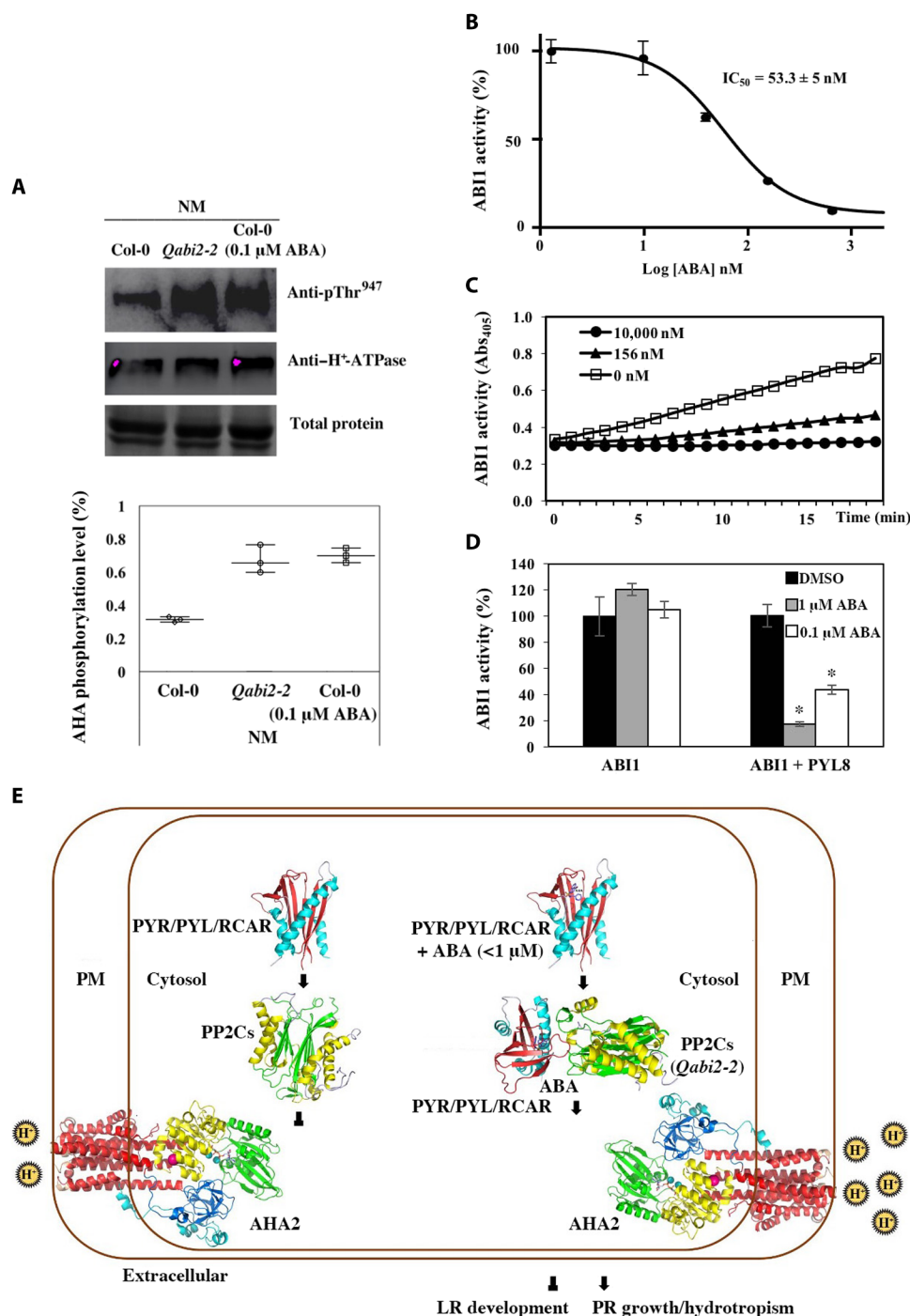
Fig. 6. Inhibition of phosphatase activity at low ABA concentrations leads to increased Thr[947] phosphorylation of AHA2. (**A**) In vivo phosphorylation level of Thr[947] in the C-terminal R domain of AHA2 in Col-0 WT either in the absence or presence of 0.1 μM ABA, and *Qabi2-2* plants grown in normal medium. The phosphorylation level of the Thr[947] in the C-terminal R domain was determined by immunoblotting using pThr[947] antibody. The phosphorylation level of AHA was quantified as the ratio of the signal intensity from the phosphorylated AHA to that from the amount of AHA (graph at middle). These assays were repeated at least three times with similar results. (**B** to **D**) In vitro phosphatase assay showed inhibition of ABI1 activity by PYL8 at low ABA concentration. (B) The half-maximal inhibitory concentration (IC$_{50}$) for ABI1 in the presence of PYL8 was calculated using different ABA concentrations. (C) Kinetic analysis of ABI1 activity for 20 min in the presence of PYL8 and the indicated ABA concentrations. Abs$_{405}$, absorbance at 405 nm. (D) End point activity of ABI1 after 30-min incubation. The asterisks indicate a significant difference based on the Student's t test (*$P < 0.05$). (**E**) Model of ABI1-mediated PM H$^+$ extrusion through interaction with AHA2. AHA2 represented as a transmembrane protein, which located into PM. In the absence of ABA (left), apo-PYL1 receptor [Protein Data Bank (PDB) code: 3KAY] does not interact with ABI1. Therefore, ABI1 interacts with and dephosphorylates the C-terminal R domain of AHA2. In the presence of low concentrations of ABA (right), the PYL1 receptor is in a complex with ABI1 phosphatase (PDB code: 3JRQ). Hence, ABI1 is unable to interact with and dephosphorylate AHA2. Then, AHA2 maintains in the phosphorylated state and promotes root growth and hydrotropism through apoplastic acidification.

Application of high ABA concentration (10 μM) decreases apoplastic H$^+$ extrusion and leads to inhibition of root growth in *Arabidopsis* (*29*), and Hayashi *et al.* (*30*) reported that application of 20 μM ABA induces dephosphorylation of Thr^{947} in AHA and suppresses hypocotyl elongation in an ABI1-dependent manner. Application of high ABA concentrations for several hours leads to up-regulation of transcripts and protein levels of PP2Cs (*69*, *70*). The increase in protein levels of PP2Cs acts as a negative feedback mechanism to reset ABA signaling, and according to our results, we suggest that it will reduce the phosphorylation level of Thr^{947} and inhibit apoplastic H$^+$ extrusion. In this study, however, we analyzed the phosphorylation status of AHA2 in the WT in the presence of low ABA concentration (0.1 μM), and we found enhanced phosphorylation of Thr^{947} compared to mock-treated plants. In accordance with this result, supplementing the medium with 0.1 μM ABA results in longer root phenotype and higher apoplastic H$^+$ extrusion compared to nonsupplemented medium.

On the basis of our findings, we propose a working model to explain the effect of low ABA concentrations (<1.0 μM) on AHA2 activity and root growth (Fig. 6E). When PP2Cs are active, they form a complex with AHA2 and dephosphorylate Thr^{947} to suppress H$^+$ efflux (Fig. 6E, left). Under moderate water stress or in the presence of low ABA concentrations, cytosolic ABA receptors bind to PP2Cs to relieve AHA2, resembling the phenotype of *Qabi2-2* plants. Therefore, either by ABA-dependent inhibition or genetic inactivation of PP2Cs, Thr^{947} in the C terminus of AHA is maintained in the phosphorylated state, which activates apoplastic H$^+$ extrusion (Fig. 6E, right). Figure 6 (B to D) shows that ABI1 phosphatase activity is down-regulated in the presence of PYL8/RCAR3 at low ABA concentrations, and genetic support for this model is provided in Fig. 6A through the analysis of Thr^{947} phosphorylation in *Qabi2-2* plants or WT treated with 0.1 μM ABA (Fig. 6, A to C). Furthermore, combined with the previous key finding that MIZ1 and the ABA-activated SnRK2.2 kinase act coordinately in elongation zone cortical cells for hydrotropism (*25*), we conclude that inhibition of PP2Cs and promotion of AHA activity in the root elongation zone play a critical role in the hydrotropic response of *Arabidopsis* roots, together with the capital effects of SnRK2.2 and MIZ1 (fig. S9).

In summary, we found that PP2Cs interact with the C terminus of AHA2 and ABI1 dephosphorylates Thr^{947}, leading to decreased H$^+$ efflux, lower primary root growth, and compromised root hydrotropism. In contrast, BRI1 might be a positive regulator of AHA activity because it was reported to bind AHA2 and AHA7, and the *bri1-5* loss-of-function mutant displays impaired primary root growth and reduced hydrotropism, as well as decreased apoplastic H$^+$ efflux (*48*, *49*, *77*, *78*). Together, we suggest that PM H$^+$ extrusion is crucial for primary root growth and the hydrotropic response in *Arabidopsis* roots, which is regulated by several phytohormones. Auxin-induced growth is characterized by acidification of the cell wall, which results in cellular expansion and cell elongation (*79*). Auxin-induced small auxin up-RNA proteins inhibit PP2CD subfamily of PP2Cs, which negatively regulate PM AHA activity, and therefore, auxin stimulates PM AHA activity through promoting phosphorylation of Thr^{947} (*80*). Here, we found that clade A PP2C ABI1 involved in ABA signaling also dephosphorylates Thr^{947} of the PM AHA. As a result, the activation of the PM AHA maintained in the phosphorylated state by auxin or low ABA concentrations could be reverted by high ABA concentrations.

MATERIALS AND METHODS

Plant material and growth conditions
Seeds of *Arabidopsis thaliana* ecotype Col-0 WT, *aha2* (AT4G30190), ABA-related mutants, *aba1-1* (AT5G67030), *aba2-1* (AT1G52340), *cyp707a-1* (AT2G29090), *112458* (AT4G17870, AT5G46790, AT2G26040, AT2G38310, AT5G05440, and AT5G53160), *abi1-3*, *hab1-1abi1-2abi2-2*, *hab1-1abi1-2pp2ca-1*, and quadruple mutant *Qabi2-2* (*hab1-1abi1-2pp2ca-1abi2-2*; AT1G72770, AT4G26080, AT3G11410, and AT5G57050) were first surface-sterilized with 100% bleach for 3 min, washed five times with sterile water, and then sown on plates containing one-half–strength Murashige and Skoog (MS) medium supplemented with 1% (w/v) sucrose and 0.8% (w/v) agarose. *aha2*, *aba1-1*, *aba2-1*, *cyp707a2-1*, *112458*, *abi1-3*, *hab1-1abi1-2abi2-2*, *hab1-1abi1-2pp2ca-1*, and *Qabi2-2* mutants are in Col-0 background. Plates were held at 4°C for 2 days for vernalization. Then, the materials were grown vertically for 5 days and transferred to one-half–strength Hoagland medium (normal medium) and one-half–strength Hoagland medium containing 0.3% (v/v) glycerol and 0.06% (w/v) alginic acid in a water potential gradient assay (water stress medium) according to Miao *et al.* (*48*), without (mock) or with 0.1, 3, or 10 μM ABA for vertical growth lasting other 2 or 5 days, respectively, or transferred to one-half–strength MS medium supplemented with 400 mM D-sorbitol for vertical growth lasting 12 or 16 hours, in an obliquely oriented hydrotropic experimental system, described by Miao *et al.* (*48*). The water potentials of normal medium and water stress medium were measured according to Miao *et al.* (*48*). The plants were placed in growth chambers at dark/light cycles [8-hour dark (21°C) and 16-hour light (23°C)].

RNA-seq assay
Total RNA was extracted from the root tips of Col-0 seedlings at 7 dag in normal medium and water stress medium, using the TRIzol reagent (Invitrogen, Carlsbad, CA, USA) in accordance with the manufacturer's protocol. First-strand complementary DNA (cDNA) was prepared by an EasyScript One-Step gDNA Removal and cDNA Synthesis SuperMix (TransGen Biotech) with random hexamers. Sequencing was performed using the HiSeq 2000 System located at the Beijing Genomics Institute, including two kinds of treatment processing, Col-0 (normal medium) (seedling grown in normal medium) and Col-0 (water stress medium) (seedlings grown in water stress medium). The RNA-seq data used in the study were deposited in the Gene Expression Omnibus (www.ncbi.nlm.nih.gov/geo/) under code PRJNA605515 (*56*).

H$^+$ efflux assay
H$^+$ fluxes in *Arabidopsis* primary roots and lateral roots were measured using the scanning ion selective electrode technique (SIET system BIO-003A, Younger USA Science and Technology) according to Xu *et al.* (*81*).

AHA activity and H$^+$ transport assays
PM proteins and vesicles were isolated from 7-dag Col-0 WT and *Qabi2-2* roots according to Zhu *et al.* (*82*) with minor modifications. PM protein content was calculated using the Bradford assay. Ten micrograms of PM proteins were used to determine the AHA activities by measuring the release of Pi from ATP according to the method of Kinoshita and Shimazaki (*43*) using an ultraviolet (UV) spectrophotometer (Spectramax 250, Molecular Devices, Sunnyvale, CA, USA)

under the reaction temperature 30°C. The H$^+$ transport activity was measured as the quenching of A$_{492}$ by acridine orange after adding a mixture of Mg-ATP (MgSO$_4$ and disodium ATP) at a final concentration of 1 mM using a UV spectrophotometer (Spectramax 250, Molecular Devices, Sunnyvale, CA, USA) under the reaction temperature 30°C according to the method of Zhu *et al.* (*82*). To determine the PM purity, AHA activity was monitored in the amount of released Pi with or without specific inhibitors including sodium VA (0.02 mM; pH 6.5) for PM, nitrate (50 mM; pH 8) for tonoplast, and azide (1 mM; pH 8) for mitochondrial and endoplasmic membrane according to the method of Zhu *et al.* (*82*). Each experiment was repeated three times, independently.

Split-ubiquitin Y2H assay
For split-ubiquitin Y2H assay, the full-length coding regions of *AHA2* and *ABI1* were subcloned into pBT3-N Cub (including the C-terminal half of ubiquitin) and pPR3-N NubG (including the N-terminal half of ubiquitin) vectors to yield fusion constructs, respectively. The experiments were performed as described previously (*83*). Primers are listed in table S3.

BiFC assay
For BiFC assay, the amplified polymerase chain reaction products of full-length ABI1, HAB1, PP2CA, and AHA2 coding DNA sequences were subcloned into pCAMBIA1300-N1-YFPC and pCAMBIA1300-N1-YFPN vectors to yield cYFP and nYFP fusion constructs, respectively. The BiFC assay were performed as described previously (*48*, *49*). The YFP fluorescence images were obtained using a Leica SP8 confocal laser scanning microscope (Leica, Heidelberg, Germany). The primers used are listed in table S3.

Y2H assay
The truncated derivatives coding sequences of *AHA2* were subcloned into pGADT7, and the full-length *ABI1* coding sequence was subcloned into pGBKT7. Y2H assays were performed according to the Matchmaker Gold Yeast Two-Hybrid System manual (Clontech). The constructs for each pair were cotransformed into yeast (*Saccharomyces cerevisiae*) strain AH109. The cotransformed yeast cells were eventually grown on SD (synthetically defined)–Lue-Trp-His-Ade plates to identify the protein-protein interactions using two reporter genes, *His3* and *Ade2*. All primers used for plasmid construction are listed in table S3.

Firefly LCI assay
For LCI assay, the full-length *ABI1* coding sequences were subcloned into the *pCAMBIA-1300NLuc* vector using Kpn I and Spe I sites, and the C-terminal R domain coding sequences of *AHA2* were subcloned into *pCAMBIA-1300CLuc* vector using Kpn I and Spe I sites, respectively. These constructs were cotransformed into *Agrobacterium* strain GV3101 and infiltrated into *N. benthamiana* leaves. After 2 days, the infiltrated *N. benthamiana* leaves were treated with 1 mM D-luciferin (Promega, catalog number E160A) and maintained in darkness for 5 min, and a low-light cooled 644 charge-coupled device camera (ikon-L936, Andor Tech) were used to detect the luciferase (LUC) signals. Primers are listed in table S3.

AHA phosphorylation assay
For dephosphorylation assays, either ABI1-GFP or GFP was coexpressed with the C-terminal domain of *AHA2* in *N. benthamiana*

leaves. To this end, the full-length *ABI1* coding sequence was subcloned into *BWA(V)HS-GFP* vector using a Bsa I/Eco31 I site, whereas the C-terminal domain of *AHA2* was subcloned into *pCAMBIA1306-Flag (3×)* vector using Kpn I and Spe I sites, respectively. Then, these constructs were cotransformed into *Agrobacterium* strain GV3101 and infiltrated into *N. benthamiana* leaves. After 1 day, the isolated cytosolic protein fractions were mixed with protein extracts prepared from an *Arabidopsis G-box regulating factor 6* (*GRF6*) (AT5G10450) overexpression transgenic line, a member of the 14-3-3 gene family. The phosphorylation level of the penultimate threonine in the C-terminal domain was determined by immunoblot analysis using antibodies against pThr^{947} according to Hayashi *et al.* (*30*, *64*). For Col-0 WT, *miz1* and quadruple mutant *Qabi2-2* phosphorylation assays, the samples of Col-0 WT in the presence or absence of 0.1 μM ABA, *miz1*, and quadruple mutant *Qabi2-2* seedlings grown on normal medium were prepared and collected as mentioned above. The PM fractions were isolated from indicated *Arabidopsis* roots according to Spartz *et al.* (*80*) and collected according to Zhu *et al.* (*82*). Immunoblot analysis was conducted according to Hayashi *et al.* (*30*, *64*) with minor modifications for *Arabidopsis* roots. Primers are listed in table S3.

PP2C inhibition assay
Phosphatase activity was assayed using *p*-nitrophenyl phosphate as a substrate according to Belda-Palazon *et al.* (*68*). To calculate PP2C activity, the final absorbance value was substracted from the initial value and was expressed as percentage of phosphatase activity in the absence of ABA. Three independent experiments were performed, and values are averages ± SD. Asterisk indicates *P* < 0.05 (Student's *t* test) when comparing data of ABI1 samples incubated with PYL8 and ABA versus PYL8 in the absence of ABA. Dimethyl sulfoxide (DMSO) wells contain 1% (v/v) DMSO and correspond to 100% of phosphatase activity.

HPTS staining and confocal imaging
HPTS staining was performed by incubating 5-dag Col-0 WT root transferred to normal medium or obliquely oriented hydrotropic experimental system lasting 2 or 16 hours for 30 min in one-half–strength MS liquid growth medium supplemented with 1 mM HPTS and 0.01% (v/v) Silwet L-77. Root curvature imaging was observed using Leica SP8 confocal laser scanning microscope (Leica, Heidelberg, Germany). Fluorescent signals for the protonated HPTS form (deep blue) (excitation, 405 nm) and deprotonated HPTS form (light blue) (excitation, 458 nm) were detected with a 40× objective (water immersion) under the same emission peak of 514 nm according to Barbez *et al.* (*62*). Fiji software (http://fiji.sc/) was used to analyze the images, and the experiments in the study were conducted at least three biological repetitions.

Homology modeling
Cartoon representations of AHA2, apo-PYL1, ABI1, and PYL1-ABA-ABI1 crystal structures were drawn by the software PyMOL (www.pymol.org). The x-ray crystal structures of AHA2 [Protein Data Bank (PDB) code: 1RT8], apo-PYL1 (PDB code: 3KAY), and PYL1-ABA-ABI1 (PDB code: 3JRQ) served as the structural templates. The tertiary structural model of C terminus of AHA2 was created by the program MODELLER (http://salilab.org/modeller/). The x-ray cocrystal structure of the 14-3-3/AHA plant complex (PDB code: 2O98) served as templates for homology modeling (*84–86*).

Measurement of ABA

ABA contents in 10-dag Col-0 with or without 0.1 and 3 µM ABA, *miz1* mutant with or without 0.1 µM ABA, and *Qabi2-2* seedlings grown on normal medium were measured by Wuhan Metware Biotechnology Co. Ltd. (Wuhan, China) (www.metware.cn/) based on the AB Sciex QTRAP 6500 liquid chromatography (LC)–MS/MS platform, according to Chen *et al.* (*87*).

LC-MS/MS analysis

pCAMBIA1306–AHA2 (C100)–Flag (3×) vector was transformed and expressed in *N. benthamiana*, and AHA2 (C100)–FLAG (3×) was purified by affinity chromatography using the FLAG-tag for MS. The LC-MS/MS spectra were analyzed by Shanghai Applied Protein Technology Co. Ltd. (Shanghai, China) according to Zhou *et al.* (*88*).

Statistical analysis

Data were analyzed by the Statistical Package for Social Sciences. The mean difference was analyzed by Student's *t* test or one-way analysis of variance (ANOVA) using the Tukey's post hoc test.

SUPPLEMENTARY MATERIALS

Supplementary material for this article is available at http://advances.sciencemag.org/cgi/content/full/7/12/eabd4113/DC1

View/request a protocol for this paper from *Bio-protocol*.

REFERENCES AND NOTES

1. C. S. Galvan-Ampudia, M. M. Julkowska, E. Darwish, J. Gandullo, R. A. Korver, G. Brunoud, M. A. Haring, T. Munnik, T. Vernoux, C. Testerink, Halotropism is a response of plant roots to avoid a saline environment. *Curr. Biol.* **23**, 2044–2050 (2013).
2. N. E. Robbins II, C. Trontin, L. Duan, J. R. Dinneny, Beyond the barrier: Communication in the root through the endodermis. *Plant Physiol.* **166**, 551–559 (2014).
3. M. M. Julkowska, I. T. Koevoets, S. Mol, H. Hoefsloot, R. Feron, M. A. Tester, J. J. B. Keurentjes, A. Korte, M. A. Haring, G.-J. de Boer, C. Testerink, Genetic components of root architecture remodeling in response to salt stress. *Plant Cell* **29**, 3198–3213 (2017).
4. Y. Zhao, T. Wang, W. Zhang, X. Li, SOS3 mediates lateral root development under low salt stress through regulation of auxin redistribution and maxima in Arabidopsis. *New Phytol.* **189**, 1122–1134 (2011).
5. Y. Bao, P. Aggarwal, N. E. Robbins II, C. J. Sturrock, M. C. Thompson, H. Q. Tan, C. Tham, L. Duan, P. L. Rodriguez, T. Vernoux, S. J. Mooney, M. J. Bennett, J. R. Dinneny, Plant roots use a patterning mechanism to position lateral root branches toward available water. *Proc. Natl. Acad. Sci. U.S.A.* **111**, 9319–9324 (2014).
6. B. Orman-Ligeza, E. C. Morris, T. Parizot, T. Lavigne, A. Babé, A. Ligeza, S. Klein, C. Sturrock, W. Xuan, O. Novák, K. Ljung, M. A. Fernandez, P. L. Rodriguez, I. C. Dodd, I. De Smet, F. Chaumont, H. Batoko, C. Périlleux, J. P. Lynch, M. J. Bennett, T. Beeckman, X. Draye, The xerobranching response represses lateral root formation when roots are not in contact with water. *Curr. Biol.* **28**, 3165–3173.e5 (2018).
7. J. E. Malamy, K. Ryan, Environmental regulation of lateral root initiation in Arabidopsis. *Plant Physiol.* **127**, 899–909 (2001).
8. J. E. Malamy, Intrinsic and environmental response pathways that regulate root system architecture. *Plant Cell Environ.* **28**, 67–77 (2005).
9. F. A. Ditengou, W. D. Teale, P. Kochersperger, K. A. Flittner, I. Kneuper, E. van der Graaff, H. Nziengui, F. Pinosa, X. Li, R. Nitschke, T. Laux, K. Palme, Mechanical induction of lateral root initiation in *Arabidopsis thaliana*. *Proc. Natl. Acad. Sci. U.S.A.* **105**, 18818–18823 (2008).
10. M. J. Jaffe, H. Takahashi, R. L. Biro, A pea mutant for the study of hydrotropism in roots. *Science* **230**, 445–447 (1985).
11. W. Feng, H. Lindner, N. E. Robbins, J. R. Dinneny, Growing out of stress: The role of cell- and organ-scale growth control in plant water-stress responses. *Plant Cell* **28**, 1769–1782 (2016).
12. Y. Ma, I. Szostkiewicz, A. Korte, D. Moes, Y. Yang, A. Christmann, E. Grill, Regulators of PP2C phosphatase activity function as abscisic acid sensors. *Science* **324**, 1064–1068 (2009).
13. N. Nishimura, K. Hitomi, A. S. Arvai, R. P. Rambo, C. Hitomi, S. R. Cutler, J. I. Schroeder, E. D. Getzoff, Structural mechanism of abscisic acid binding and signaling by dimeric PYR1. *Science* **326**, 1373–1379 (2009).
14. N. Nishimura, A. Sarkeshik, K. Nito, S.-Y. Park, A. Wang, P. C. Carvalho, S. Lee, D. F. Caddell, S. R. Cutler, J. Chory, J. R. Yates, J. I. Schroeder, PYR/PYL/RCAR family members are major *in-vivo* ABI1 protein phosphatase 2C-interacting proteins in Arabidopsis. *Plant J.* **61**, 290–299 (2010).
15. R. Antoni, L. Rodriguez, M. Gonzalez-Guzman, G. A. Pizzio, P. L. Rodriguez, News on ABA transport, protein degradation, and ABFs/WRKYs in ABA signaling. *Curr. Opin. Plant Biol.* **14**, 547–553 (2011).
16. S.-Y. Park, P. Fung, N. Nishimura, D. R. Jensen, H. Fujii, Y. Zhao, S. Lumba, J. Santiago, A. Rodrigues, T.-F. F. Chow, S. E. Alfred, D. Bonetta, R. Finkelstein, N. J. Provart, D. Desveaux, P. L. Rodriguez, P. M. Court, J.-K. Zhu, J. I. Schroeder, B. F. Volkman, S. R. Cutler, Abscisic acid inhibits type 2C protein phosphatases via the PYR/PYL family of START proteins. *Science* **324**, 1068–1071 (2009).
17. K. Melcher, L.-M. Ng, X. E. Zhou, F.-F. Soon, Y. Xu, K. M. Suino-Powell, S.-Y. Park, J. J. Weiner, H. Fujii, V. Chinnusamy, A. Kovach, J. Li, Y. Wang, J. Li, F. C. Peterson, D. R. Jensen, E.-L. Yong, B. F. Volkman, S. R. Cutler, J.-K. Zhu, H. E. Xu, A gate-latch-lock mechanism for signal transduction by abscisic acid receptors. *Nature* **462**, 602–608 (2009).
18. J. Santiago, F. Dupeux, A. Round, R. Antoni, S.-Y. Park, M. Jamin, S. R. Cutler, P. L. Rodriguez, J. A. Márquez, The abscisic acid receptor PYR1 in complex with abscisic acid. *Nature* **462**, 665–668 (2009).
19. P. Yin, H. Fan, Q. Hao, X. Yuan, D. Wu, Y. Pang, C. Yan, W. Li, J. Wang, N. Yan, Structural insights into the mechanism of abscisic acid signaling by PYL proteins. *Nat. Struct. Mol. Biol.* **16**, 1230–1236 (2009).
20. K.-i. Miyazono, T. Miyakawa, Y. Sawano, K. Kubota, H.-J. Kang, A. Asano, Y. Miyauchi, M. Takahashi, Y. Zhi, Y. Fujita, T. Yoshida, K.-S. Kodaira, K. Yamaguchi-Shinozaki, M. Tanokura, Structural basis of abscisic acid signalling. *Nature* **462**, 609–614 (2009).
21. Y. Uno, T. Furihata, H. Abe, R. Yoshida, K. Shinozaki, K. Yamaguchi-Shinozaki, *Arabidopsis* basic leucine zipper transcription factors involved in an abscisic acid-dependent signal transduction pathway under drought and high-salinity conditions. *Proc. Natl. Acad. Sci. U.S.A.* **97**, 11632–11637 (2000).
22. T. Furihata, K. Maruyama, Y. Fujita, T. Umezawa, R. Yoshida, K. Shinozaki, K. Yamaguchi-Shinozaki, Abscisic acid-dependent multisite phosphorylation regulates the activity of a transcription activator AREB1. *Proc. Natl. Acad. Sci. U.S.A.* **103**, 1988–1993 (2006).
23. H. Fujii, P. E. Verslues, J.-K. Zhu, Identification of two protein kinases required for abscisic acid regulation of seed germination, root growth, and gene expression in *Arabidopsis*. *Plant Cell* **19**, 485–494 (2007).
24. R. Antoni, M. Gonzalez-Guzman, L. Rodriguez, M. Peirats-Llobet, G. A. Pizzio, M. A. Fernandez, N. De Winne, D. De Jaeger, D. Dietrich, M. J. Bennett, P. L. Rodriguez, PYRABACTIN RESISTANCE1-LIKE8 plays an important role for the regulation of abscisic acid signaling in root. *Plant Physiol.* **161**, 931–941 (2013).
25. D. Dietrich, L. Pang, A. Kobayashi, J. A. Fozard, V. Boudolf, R. Bhosale, R. Antoni, T. Nguyen, S. Hiratsuka, N. Fujii, Y. Miyazawa, T.-W. Bae, D. M. Wells, M. R. Owen, L. R. Band, R. J. Dyson, O. E. Jensen, J. R. King, S. R. Tracy, C. J. Sturrock, S. J. Mooney, J. A. Roberts, R. P. Bhalerao, J. R. Dinneny, P. L. Rodriguez, A. Nagatani, Y. Hosokawa, T. I. Baskin, T. P. Pridmore, I. De Veylder, H. Takahashi, M. J. Bennett, Root hydrotropism is controlled via a cortex-specific growth mechanism. *Nat Plants* **3**, 17057 (2017).
26. N. Takahashi, N. Goto, K. Okada, H. Takahashi, Hydrotropism in abscisic acid, wavy, and gravitropic mutants of *Arabidopsis thaliana*. *Planta* **216**, 203–211 (2002).
27. D. Eapen, Ḿ. L. Barroso, Ḿ. E. Campos, G. Ponce, G. Corkidi, J. G. Dubrovsky, G. I. Cassab, *A no hydrotropic response* root mutant that responds positively to gravitropism in Arabidopsis. *Plant Physiol.* **131**, 536–546 (2003).
28. T. Moriwaki, Y. Miyazawa, N. Fujii, H. Takahashi, Light and abscisic acid signalling are integrated by *MIZ1* gene expression and regulate hydrotropic response in roots of *Arabidopsis thaliana*. *Plant Cell Environ.* **35**, 1359–1368 (2012).
29. M. D. Planes, R. Niñoles, L. Rubio, G. Bissoli, E. Bueso, M. J. García-Sánchez, S. Alejandro, M. Gonzalez-Guzmán, R. Hedrich, P. L. Rodriguez, J. A. Fernández, R. Serrano, A mechanism of growth inhibition by abscisic acid in germinating seeds of *Arabidopsis thaliana* based on inhibition of plasma membrane H⁺-ATPase and decreased cytosolic pH, K⁺, and anions. *J. Exp. Bot.* **66**, 813–825 (2015).
30. Y. Hayashi, K. Takahashi, S. Inoue, T. Kinoshita, Abscisic acid suppresses hypocotyl elongation by dephosphorylating plasma membrane H⁺-ATPase in *Arabidopsis thaliana*. *Plant Cell Physiol.* **55**, 845–853 (2014).
31. J. Falhof, J. T. Pedersen, A. T. Fuglsang, M. Palmgren, Plasma membrane H⁺-ATPase regulation in the center of plant physiology. *Mol. Plant* **9**, 323–337 (2016).
32. M. Haruta, W. M. Gray, M. R. Sussman, Regulation of the plasma membrane proton pump (H⁺-ATPase) by phosphorylation. *Curr. Opin. Plant Biol.* **28**, 68–75 (2015).
33. K. Ekberg, M. G. Palmgren, B. Veierskov, M. J. Buch-Pedersen, A novel mechanism of P-type ATPase autoinhibition involving both termini of the protein. *J. Biol. Chem.* **285**, 7344–7350 (2010).
34. F. Svennelid, A. Olsson, M. Piotrowski, M. Rosenquist, C. Ottman, C. Larsson, C. Oecking, M. Sommarin, Phosphorylation of Thr-948 at the C terminus of the plasma membrane

H^{+}-ATPase creates a binding site for the regulatory 14-3-3 protein. *Plant Cell* **11**, 2379–2391 (1999).

35. K. Takahashi, K.-i. Hayashi, T. Kinoshita, Auxin activates the plasma membrane H^{+}-ATPase by phosphorylation during hypocotyl elongation in Arabidopsis. *Plant Physiol.* **159**, 632–641 (2012).

36. A. T. Fuglsang, S. Visconti, K. Drumm, T. Jahn, A. Stensballe, B. Mattei, O. N. Jensen, P. Aducci, M. G. Palmgren, Binding of 14-3-3 protein to the plasma membrane H+-ATPase AHA2 involves the three C-terminal residues Tyr946-Thr-Val and requires phosphorylation of Thr947. *J. Biol. Chem.* **274**, 36774–36780 (1999).

37. L. Camoni, V. Iori, M. Marra, P. Aducci, Phosphorylation-dependent interaction between plant plasma membrane H^{+}-ATPase and 14-3-3 proteins. *J. Biol. Chem.* **275**, 9919–9923 (2000).

38. F. Gévaudant, G. Duby, S. E. Von, R. Zhao, P. Morsomme, M. Boutry, Expression of a constitutively activated plasma membrane H^{+}-ATPase alters plant development and increases salt tolerance. *Plant Physiol.* **144**, 1763–1776 (2007).

39. A. T. Fuglsang, J. Borch, K. Bych, T. P. Jahn, P. Roepstorff, M. G. Palmgren, The binding site for regulatory 14-3-3 protein in plant plasma membrane H^{+}-ATPase: Involvement of a region promoting phosphorylation-independent interaction in addition to the phosphorylation-dependent C-terminal end. *J. Biol. Chem.* **278**, 42266–42272 (2003).

40. O. Maudoux, H. Batoko, C. Oecking, K. Gevaert, J. Vandekerckhove, M. Boutry, P. Morsomme, A plant plasma membrane H^{+}-ATPase expressed in yeast is activated by phosphorylation at its penultimate residue and binding of 14-3-3 regulatory proteins in the absence of fusicoccin. *J. Biol. Chem.* **275**, 17762–17770 (2000).

41. J. Kanczewska, S. Marco, C. Vandermeeren, O. Maudoux, J. L. Rigaud, M. Boutry, Activation of the plant plasma membrane H^{+}-ATPase by phosphorylation and binding of 14-3-3 proteins converts a dimer into a hexamer. *Proc. Natl. Acad. Sci. U.S.A.* **102**, 11675–11680 (2005).

42. A. T. Fuglsang, Y. Guo, T. A. Cuin, Q. Qiu, C. Song, K. A. Kristiansen, K. Bych, A. Schulz, S. Shabala, K. S. Schumaker, M. G. Palmgren, J. K. Zhu, *Arabidopsis* protein kinase PKS5 inhibits the plasma membrane H^{+}-ATPase by preventing interaction with 14-3-3 protein. *Plant Cell* **19**, 1617–1634 (2007).

43. T. Kinoshita, K.-i. Shimazaki, Biochemical evidence for the requirement of 14-3-3 protein binding in activation of the guard-cell plasma membrane H^{+}-ATPase by blue light. *Plant Cell Physiol.* **43**, 1359–1365 (2002).

44. Y. Yang, Y. Qin, C. Xie, F. Zhao, J. Zhao, D. Liu, S. Chen, A. T. Fuglsang, M. G. Palmgren, K. S. Schumaker, X. W. Deng, Y. Guo, The *Arabidopsis* chaperone J3 regulates the plasma membrane H^{+}-ATPase through interaction with the PKS5 kinase. *Plant Cell* **22**, 1313–1332 (2010).

45. E. Młodzińska, G. Kłobus, M. D. Christensen, A. T. Fuglsang, The plasma membrane H^{+}-ATPase AHA2 contributes to the root architecture in response to different nitrogen supply. *Physiol. Plant.* **154**, 270–282 (2015).

46. S. Merlot, N. Leonhardt, F. Fenzi, C. Valon, M. Costa, L. Piette, A. Vavasseur, B. Genty, K. Boivin, A. Müller, J. Giraudat, J. Leung, Constitutive activation of a plasma membrane H^{+}-ATPase prevents abscisic acid-mediated stomatal closure. *EMBO J.* **26**, 3216–3226 (2007).

47. Y. Wang, K. Noguchi, N. Ono, S.-i. Inoue, I. Terashima, T. Kinoshita, Overexpression of plasma membrane H^{+}-ATPase in guard cells promotes light-induced stomatal opening and enhances plant growth. *Proc. Natl. Acad. Sci. U.S.A.* **111**, 533–538 (2014).

48. R. Miao, M. Wang, W. Yuan, Y. Ren, Y. Li, N. Zhang, J. Zhang, H. J. Kronzucker, W. Xu, Comparative analysis of Arabidopsis ecotypes reveals a role for brassinosteroids in root hydrotropism. *Plant Physiol.* **176**, 2720–2736 (2018).

49. W. Yuan, Y. Li, L. Li, W. Siao, Q. Zhang, Y. Zhang, J. Liu, W. Xu, R. Miao, BR-INSENSITIVE1 regulates hydrotropic response by interacting with plasma membrane H^{+}-ATPases in Arabidopsis. *Plant Signal. Behav.* **13**, e1486147 (2018).

50. M. Saucedo, G. Ponce, M. E. Campos, D. Eapen, E. García, R. Luján, Y. Sánchez, G. I. Cassab, An *altered hydrotropic response (ahr1)* mutant of *Arabidopsis* recovers root hydrotropism with cytokinin. *J. Exp. Bot.* **63**, 3587–3601 (2012).

51. M. Koornneef, M. L. Jorna, D. L. Brinkhorst-van der Swan, C. M. Karssen, The isolation of abscisic acid (ABA) deficient mutants by selection of induced revertants in non-germinating gibberellin sensitive lines of *Arabidopsis thaliana* (L.) heynh. *Theor. Appl. Genet.* **61**, 385–393 (1982).

52. E. Marin, L. Nussaume, A. Quesada, M. Gonneau, B. Sotta, P. Hugueney, A. Frey, A. Marion-Poll, Molecular identification of zeaxanthin epoxidase of Nicotiana plumbaginifolia, a gene involved in abscisic acid biosynthesis and corresponding to the ABA locus of Arabidopsis thaliana. *EMBO J.* **5**, 2331–2342 (1996).

53. M. González-Guzmán, N. Apostolova, J. M. Bellés, J. M. Barrero, P. Piqueras, M. R. Ponce, J. L. Micol, R. Serrano, P. L. Rodríguez, The short-chain alcohol dehydrogenase ABA2 catalyzes the conversion of xanthoxin to abscisic aldehyde. *Plant Cell* **14**, 1833–1846 (2002).

54. M. Gonzalez-Guzman, G. A. Pizzio, R. Antoni, F. Vera-Sirera, E. Merilo, G. W. Bassel, M. A. Fernández, M. J. Holdsworth, M. A. Perez-Amador, H. Kollist, P. L. Rodriguez,

Arabidopsis PYR/PYL/RCAR receptors play a major role in quantitative regulation of stomatal aperture and transcriptional response to abscisic acid. *Plant Cell* **24**, 2483–2496 (2012).

55. T. Matakiadis, A. Alboresi, Y. Jikumaru, K. Tatematsu, O. Pichon, J.-P. Renou, Y. Kamiya, E. Nambara, H.-N. Truong, The Arabidopsis abscisic acid catabolic gene *CYP707A2* plays a key role in nitrate control of seed dormancy. *Plant Physiol.* **149**, 949–960 (2009).

56. W. Yuan, Q. Zhang, Y. Li, Q. Wang, F. Xu, X. Dang, W. Xu, J. Zhang, R. Miao, Abscisic acid is required for root elongation associated with Ca^{2+} influx in response to water stress. *Front. Plant Sci.* **11**, 332 (2020).

57. E. Pacifici, R. Di Mambro, R. Dello Ioio, P. Costantino, S. Sabatini, Acidic cell elongation drives cell differentiation in the *Arabidopsis* root. *EMBO J.* **37**, e99134 (2018).

58. C. J. Griffith, P. A. Rea, E. Blumwald, R. J. Poole, Mechanism of stimulation and inhibition of tonoplast H^{+}-ATPase of *Beta vulgaris* by chloride and nitrate. *Plant Physiol.* **81**, 120–125 (1986).

59. M. W. Bowler, M. G. Montgomery, A. G. Leslie, J. E. Walker, How azide inhibits ATP hydrolysis by the F-ATPases. *Proc. Natl. Acad. Sci. U.S.A.* **103**, 8646–8649 (2006).

60. D. Shkolnik, R. Nuriel, M. C. Bonza, A. Costa, H. Fromm, MIZ1 regulates ECA1 to generate a slow, long-distance phloem-transmitted Ca^{2+} signal essential for root water tracking in *Arabidopsis*. *Proc. Natl. Acad. Sci. U.S.A.* **115**, 8031–8036 (2018).

61. J. Chang, X. Li, W. Fu, J. Wang, Y. Yong, H. Shi, Z. Ding, H. Kui, X. Gou, K. He, J. Li, Asymmetric distribution of cytokinins determines root hydrotropism in *Arabidopsis thaliana*. *Cell Res.* **29**, 984–993 (2019).

62. E. Barbez, K. Dünser, A. Gaidora, T. Lendl, W. Busch, Auxin steers root cell expansion via apoplastic pH regulation in *Arabidopsis thaliana*. *Proc. Natl. Acad. Sci. U.S.A.* **114**, E4884–E4893 (2017).

63. J. J. Weiner, F. C. Peterson, B. F. Volkman, S. R. Cutler, Structural and functional insights into core ABA signaling. *Curr. Opin. Plant Biol.* **13**, 495–502 (2010).

64. Y. Hayashi, S. Nakamura, A. Takemiya, Y. Takahashi, K.-i. Shimazaki, T. Kinoshita, Biochemical characterization of in vitro phosphorylation and dephosphorylation of the plasma membrane H^{+}-ATPase. *Plant Cell Physiol.* **51**, 1186–1196 (2010).

65. X. N. Wu, C. Sanchez Rodriguez, H. Pertl-Obermeyer, G. Obermeyer, W. X. Schulze, Sucrose-induced receptor kinase SIRK1 regulates a plasma membrane aquaporin in Arabidopsis. *Mol. Cell. Proteomics* **12**, 2856–2873 (2013).

66. Z. Lin, Y. Li, Z. Zhang, X. Liu, C.-C. Hsu, Y. Du, T. Sang, C. Zhu, Y. Wang, V. Satheesh, P. Pratibha, Y. Zhao, C.-P. Song, W. A. Tao, J.-K. Zhu, P. Wang, A RAF-SnRK2 kinase cascade mediates early osmotic stress signaling in higher plants. *Nat. Commun.* **11**, 613 (2020).

67. A. Schweighofer, H. Hirt, I. Meskiene, Plant PP2C phosphatases: Emerging functions in stress signaling. *Trends Plant Sci.* **9**, 236–243 (2004).

68. B. Belda-Palazon, M.-P. Gonzalez-Garcia, J. Lozano-Juste, A. Coego, R. Antoni, J. Julian, M. Peirats-Llobet, L. Rodriguez, A. Berbel, D. Dietrich, M. A. Fernandez, F. Madueño, M. J. Bennett, P. L. Rodriguez, PYL8 mediates ABA perception in the root through non-cell-autonomous and ligand-stabilization-based mechanisms. *Proc. Natl. Acad. Sci. U.S.A.* **115**, E11857–E11863 (2018).

69. X. Wang, C. Guo, J. Peng, C. Li, F. Wan, S. Zhang, Y. Zhou, Y. Yan, L. Qi, K. Sun, S. Yang, Z. Gong, J. Li, ABRE-BINDING FACTORS play a role in the feedback regulation of ABA signaling by mediating rapid ABA induction of ABA co-receptor genes. *New Phytol.* **221**, 341–355 (2019).

70. J. Julian, A. Coego, J. Lozano-Juste, J. Lechner, Q. Wu, X. Zhang, E. Merilo, B. Belda-Palazon, S.-Y. Park, S. R. Cutler, C. An, P. Genschik, P. L. Rodriguez, The MATH-BTB BPM3 and BPM5 subunits of Cullin3-RING E3 ubiquitin ligases target PP2CA and other clade A PP2Cs for degradation. *Proc. Natl. Acad. Sci. U.S.A.* **116**, 15725–15734 (2019).

71. M. A. Fernandez, B. Belda-Palazon, J. Julian, A. Coego, J. Lozano-Juste, S. Iñigo, L. Rodriguez, E. Bueso, A. Goossens, P. L. Rodriguez, RBR-type E3 ligases and the Ub-conjugating enzyme UBC26 regulate ABA receptor levels and signaling. *Plant Physiol.* **182**, 1723–1742 (2019).

72. S. Rubio, A. Rodrigues, A. Saez, M. B. Dizon, A. Galle, T.-H. Kim, J. Santiago, J. Flexas, J. I. Schroeder, P. L. Rodriguez, Triple loss of function of protein phosphatases type 2C leads to partial constitutive response to endogenous abscisic acid. *Plant Physiol.* **150**, 1345–1355 (2009).

73. Y. Osakabe, N. Arinaga, T. Umezawa, K. Katsura, K. Nagamachi, H. Tanaka, H. Ohiraki, K. Yamada, S.-U. Seo, M. Abo, E. Yoshimura, K. Shinozaki, K. Yamaguchi-Shinozaki, Osmotic stress responses and plant growth controlled by potassium transporters in *Arabidopsis*. *Plant Cell* **25**, 609–624 (2013).

74. T. Vahisalu, H. Kollist, Y.-F. Wang, N. Nishimura, W.-Y. Chan, G. Valerio, A. Lamminmäki, M. Brosché, H. Moldau, R. Desikan, J. I. Schroeder, J. Kangasjärvi, SLAC1 is required for plant guard cell S-type anion channel function in stomatal signalling. *Nature* **452**, 487–491 (2008).

75. B. Brandt, D. E. Brodsky, S. Xue, J. Negi, K. Iba, J. Kangasjärvi, M. Ghassemian, A. B. Stephan, H. Hu, J. I. Schroeder, Reconstitution of abscisic acid activation of SLAC1 anion channel by CPK6 and OST1 kinases and branched ABI1 PP2C phosphatase action. *Proc. Natl. Acad. Sci. U.S.A.* **109**, 10593–10598 (2012).

76. J. Negi, O. Matsuda, T. Nagasawa, Y. Oba, H. Takahashi, M. Kawai-Yamada, H. Uchiyama, M. Hashimoto, K. Iba, CO_2 regulator SLAC1 and its homologues are essential for anion homeostasis in plant cells. *Nature* **452**, 483–486 (2008).

77. N. Fàbregas, F. Lozano-Elena, D. Blasco-Escámez, T. Tohge, C. Martínez-Andújar, A. Albacete, S. Osorio, M. Bustamante, J. L. Riechmann, T. Nomura, T. Yokota, A. Conesa, F. P. Alfocea, A. R. Fernie, A. I. Caño-Delgado, Overexpression of the vascular brassinosteroid receptor BRL3 confers drought resistance without penalizing plant growth. *Nat. Commun.* **9**, 4680 (2018).

78. W. Siao, D. Coskun, F. Baluška, H. Kronzucker, W. F. Xu, Root-apex proton fluxes at the centre of soil-stress acclimation. *Trends Plant Sci.* **25**, 794–804 (2020).

79. A. Hager, Role of the plasma membrane H^+-ATPase in auxin-induced elongation growth: Historical and new aspects. *J. Plant Res.* **116**, 483–505 (2003).

80. A. K. Spartz, H. Ren, M. Y. Park, K. N. Grandt, S. H. Lee, A. S. Murphy, M. R. Sussman, P. J. Overvoorde, W. M. Gray, SAUR inhibition of PP2C-D phosphatases activates plasma membrane H^+-ATPases to promote cell expansion in *Arabidopsis*. *Plant Cell* **26**, 2129–2142 (2014).

81. W. Xu, L. Jia, W. Shi, J. Liang, F. Zhou, Q. Li, J. Zhang, Abscisic acid accumulation modulates auxin transport in the root tip to enhance proton secretion for maintaining root growth under moderate water stress. *New Phytol.* **197**, 139–150 (2013).

82. Y. Zhu, T. Di, G. Xu, X. Chen, H. Zeng, F. Yan, Q. Shen, Adaptation of plasma membrane H^+-ATPase of rice roots to low pH as related to ammonium nutrition. *Plant Cell Environ.* **32**, 1428–1440 (2009).

83. C. Grefen, P. Obrdlik, K. Harter, The determination of protein-protein interactions by the mating-based split-ubiquitin system (mbSUS). *Methods Mol. Biol.* **479**, 217–233 (2009).

84. C. Ottmann, S. Marco, N. Jaspert, C. Marcon, N. Schauer, M. Weyand, C. Vandermeeren, G. Duby, M. Boutry, A. Wittinghofer, J.-L. Rigaud, C. Oecking, Structure of a 14-3-3 coordinated hexamer of the plant plasma membrane H^+-ATPase by combining x-ray crystallography and electron cryomicroscopy. *Mol. Cell* **25**, 427–440 (2007).

85. A. Sali, L. Potterton, F. Yuan, H. van Vlijmen, M. Karplus, Evaluation of comparative protein modeling by MODELLER. *Proteins* **23**, 318–326 (1995).

86. R. Sánchez, A. Šali, Comparative protein structure modeling: Introduction and *Practical Examples with Modeller*. *Methods Mol. Bio.* **143**, 97–129 (2000).

87. W. Chen, L. Gong, Z. Guo, W. Wang, H. Zhang, X. Liu, S. Yu, L. Xiong, J. Luo, A novel integrated method for large-scale detection, identification, and quantification of widely targeted metabolites: Application in the study of rice metabolomics. *Mol. Plant* **6**, 1769–1780 (2013).

88. J. Zhou, D. Liu, P. Wang, X. Ma, W. Lin, S. Chen, K. Mishev, D. Lu, R. Kumar, I. Vanhoutte, X. Meng, P. He, E. Russinova, L. Shan, Regulation of *Arabidopsis* brassinosteroid receptor BRI1 endocytosis and degradation by plant U-box PUB12/PUB13-mediated ubiquitination. *Proc. Natl. Acad. Sci. U.S.A.* **115**, E1906–E1915 (2018).

89. P. Durek, R. Schmidt, J. L. Heazlewood, A. Jones, D. MacLean, A. Nagel, B. Kersten, W. X. Schulze, PhosPhAt: The *Arabidopsis thaliana* phosphorylation site database. An update. *Nucleic Acids Res.* **38**, D828–D834 (2010).

90. J. L. Heazlewood, P. Durek, J. Hummel, J. Selbig, W. Weckwerth, D. Walther, W. X. Schulze, PhosPhAt: A database of phosphorylation sites in *Arabidopsis thaliana* and a plant specific phosphorylation site predictor. *Nucleic Acids Res.* **36**, D1015–D1021 (2008).